Beam Line

A PERIODICAL OF PARTICLE PHYSICS

FALL/WINTER 1994 VOL. 24, NUMBER 3/4

The *Beam Line* is published quarterly by
the Stanford Linear Accelerator Center,
PO Box 4349, Stanford, CA 94309.
Telephone: (415) 926-2585
INTERNET: beamline@slac.stanford.edu
BITNET: beamline@slacvm
FAX: (415) 926-4500
SLAC is operated by Stanford University under contract with the U.S. Department of Energy. The opinions of the authors do not necessarily reflect the policy of the Stanford Linear Accelerator Center.

Cover: The structure of the Fe protein from the enzyme nitrogenase, solved by X-ray diffraction. (Photograph provided by D. C. Rees, California Institute of Technology.)

Printed on recycled paper

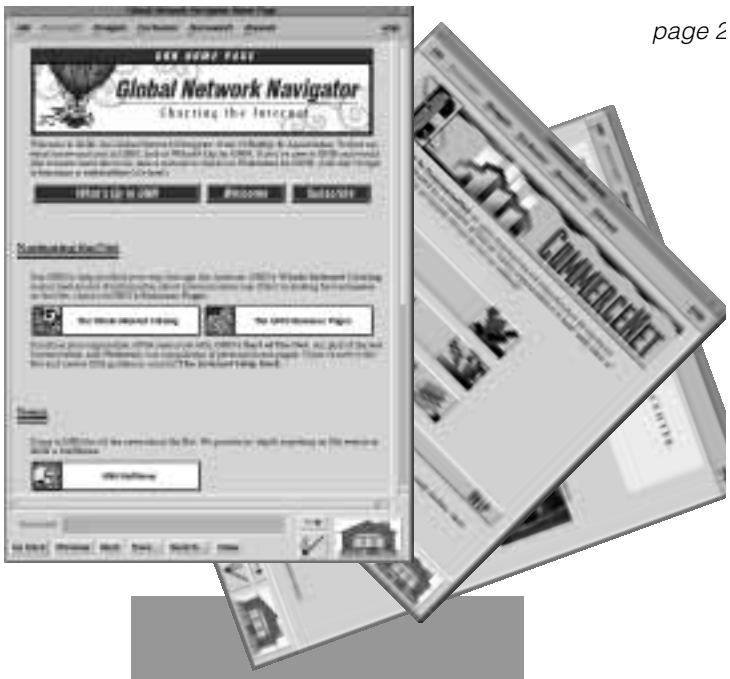

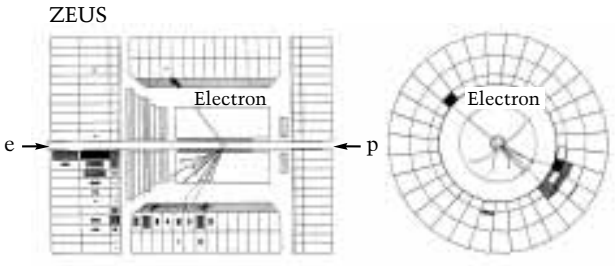

CONTENTS

FEATURES

page 10

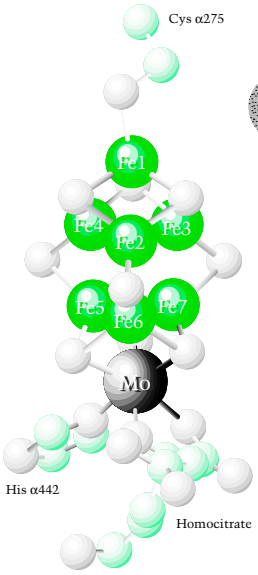

page 19

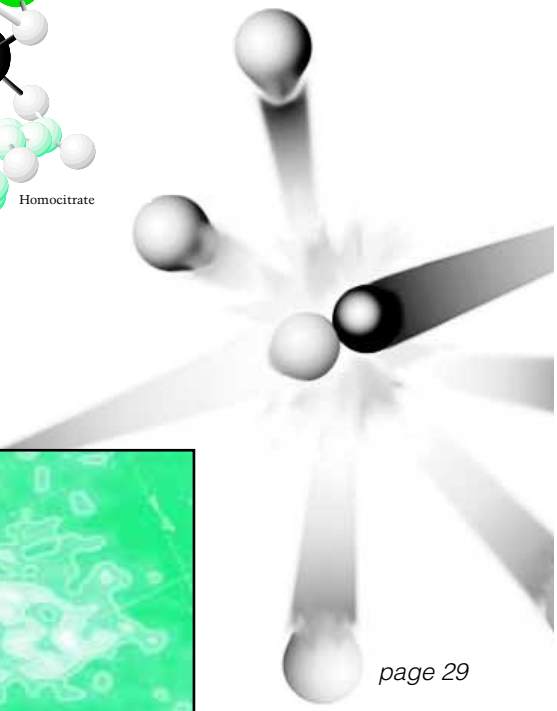

page 29

DEPARTMENTS

page 40

Spinning the World Wide Web

by TONY JOHNSON

Tony spins a tale of mystery and intrigue as he takes us on a futuristic journey around the electronic world known as "the Web."

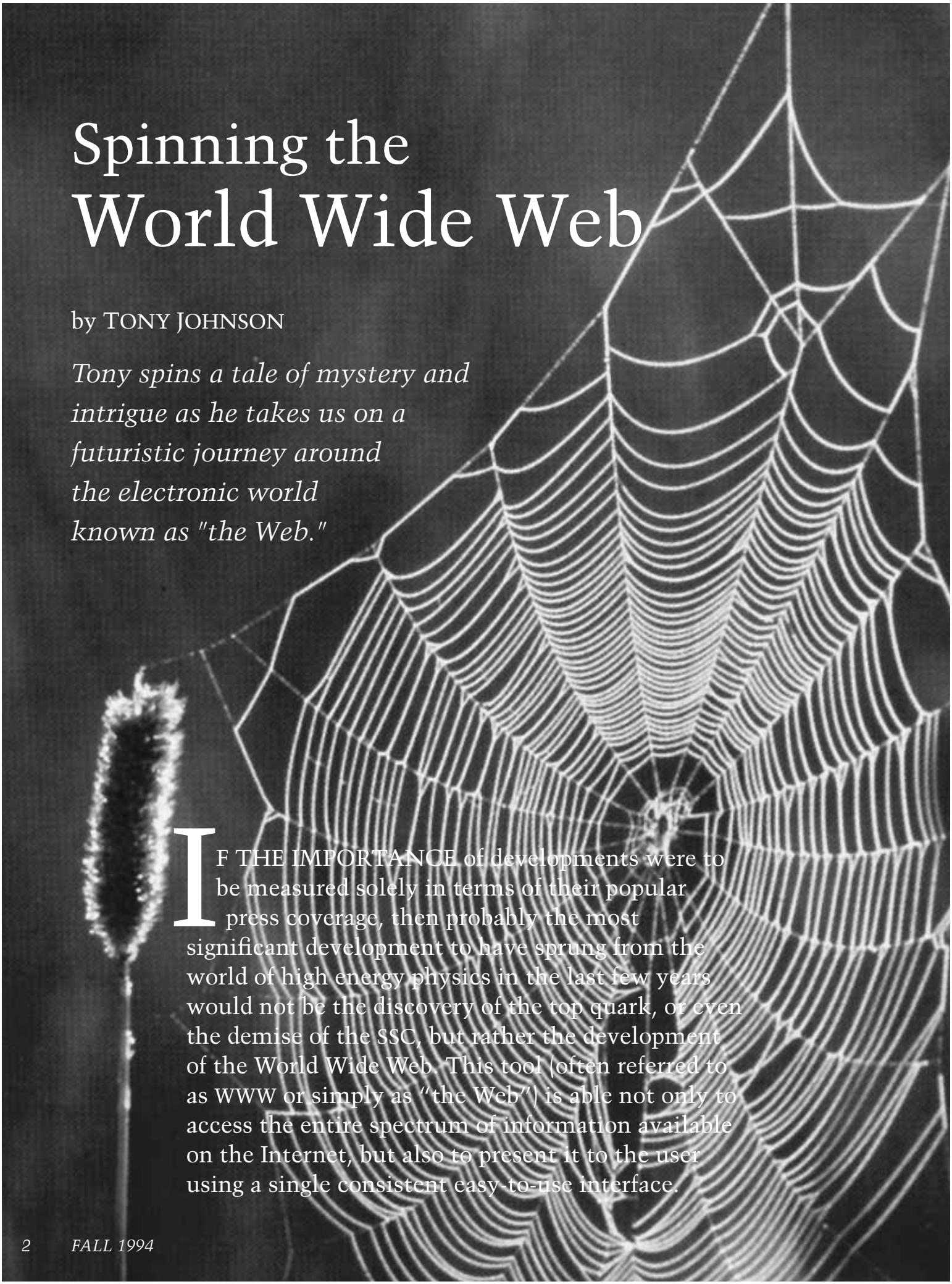

IF THE IMPORTANCE of developments were to be measured solely in terms of their popular press coverage, then probably the most significant development to have sprung from the world of high energy physics in the last few years would not be the discovery of the top quark, or even the demise of the SSC, but rather the development of the World Wide Web. This tool (often referred to as WWW or simply as "the Web") is able not only to access the entire spectrum of information available on the Internet, but also to present it to the user using a single consistent easy-to-use interface.

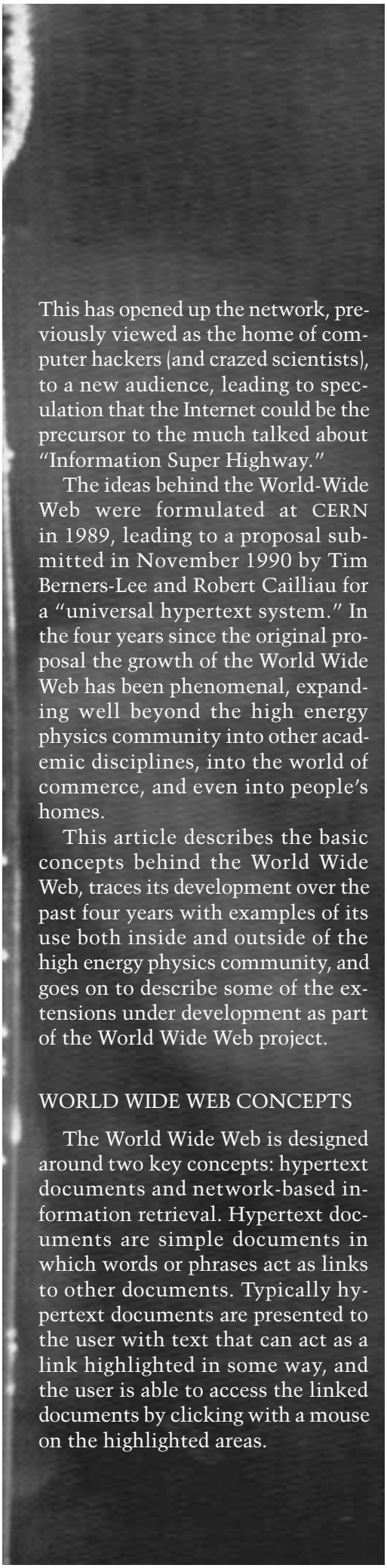

This has opened up the network, previously viewed as the home of computer hackers (and crazed scientists), to a new audience, leading to speculation that the Internet could be the precursor to the much talked about "Information Super Highway."

The ideas behind the World-Wide Web were formulated at CERN in 1989, leading to a proposal submitted in November 1990 by Tim Berners-Lee and Robert Cailliau for a "universal hypertext system." In the four years since the original proposal the growth of the World Wide Web has been phenomenal, expanding well beyond the high energy physics community into other academic disciplines, into the world of commerce, and even into people's homes.

This article describes the basic concepts behind the World Wide Web, traces its development over the past four years with examples of its use both inside and outside of the high energy physics community, and goes on to describe some of the extensions under development as part of the World Wide Web project.

WORLD WIDE WEB CONCEPTS

The World Wide Web is designed around two key concepts: hypertext documents and network-based information retrieval. Hypertext documents are simple documents in which words or phrases act as links to other documents. Typically hypertext documents are presented to the user with text that can act as a link highlighted in some way, and the user is able to access the linked documents by clicking with a mouse on the highlighted areas.

The World Wide Web extends the well-established concept of hypertext by making it possible for the destination document to be located on a completely different computer from the source document, either one located anywhere on the network. This was made possible by exploiting the existing capabilities of the Internet, a world-wide network of interconnected computers developed over the preceding 20 years, to establish a rapid connection to any named computer on the network.

To achieve this, the World Wide Web uses a client-server architecture. A user who wants to access information runs a World Wide Web client (sometimes referred to as a browser) on his local computer. The client fetches documents from remote network nodes by connecting to a server on that node and requesting the document to be retrieved. A document typically can be requested and fetched in less than a second, even when it resides on the other side of the world from the requester. (Or at least it could be in the early days of the Web; one of the drawbacks of the enormous success of the Web is that sometimes transactions are not as fast now as they were in the earlier, less heavily trafficked days. One of the challenges of the Web's future is to overcome these scaling problems.)

The client-server model offers advantages to both the information provider and the consumer. The information provider is able to keep control of the documents he maintains by keeping them on his own computer. Furthermore the documents can be maintained by the information provider in any form, so long as they can be transformed by the server software into the format the client software expects to receive. This model can naturally be extended to allow documents to be dynamically created in response to a request from users, for example by querying a database and translating the result of the query into a hypertext document.

From the information consumer's perspective, all the documents on the Web are presented in the form of hypertext. The consumer remains blissfully ignorant of how the documents are maintained by the information provider and, unless he really wants to know, from where the documents are being accessed.

GROWTH OF THE WEB

The initial implementation of the Web client at CERN was for the NeXT platform. This earliest browser was able to display documents using multiple fonts and styles and was even able to edit documents, but access was limited to users fortunate enough to have a NeXT box on their desks. This was followed by development of the CERN "linemode" browser, which could run on many platforms but which displayed its output only on character-based terminals. These early browsers were followed by the first browsers designed for X-Windows, Viola developed at the University of California, Berkeley, and Midas developed at the Stanford Linear Accelerator Center.

Initially the growth of the World Wide Web was relatively slow. By the end of 1992 there were about 50 hypertext transfer protocol (HTTP) servers. At about the same time,

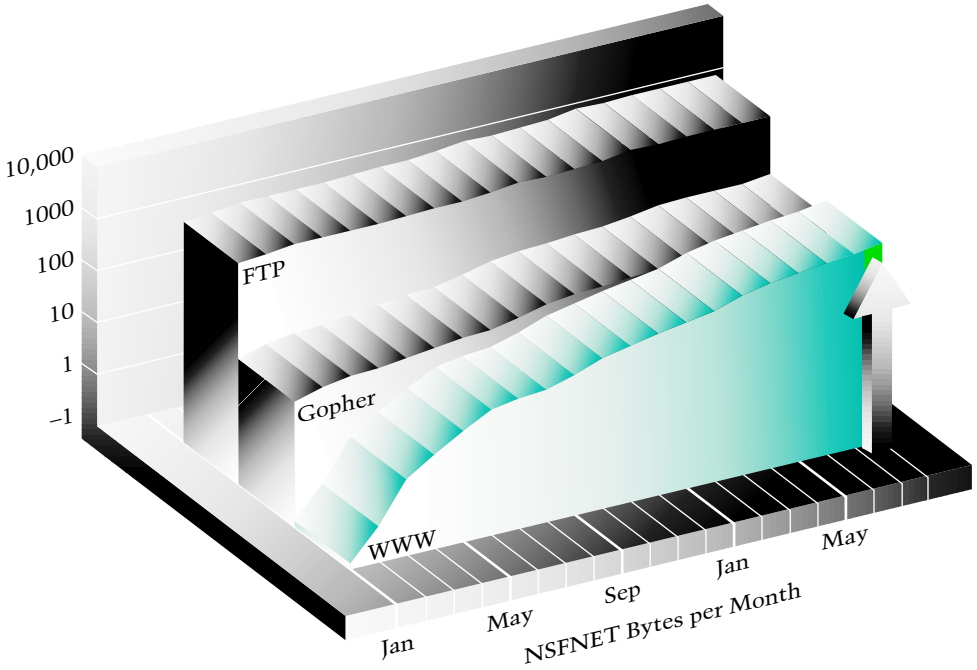

The dramatic increase of World Wide Web usage over the past year and a half is illustrated. While the growth rate is phenomenal, more traditional uses of the network such as file transfer and e-mail still dominate.

Gopher, a somewhat similar information retrieval tool to WWW but based on menus and plain text documents rather than hypertext, was expanding rapidly with several hundred servers.

During 1993 the situation changed dramatically, driven in large part by the development of the Mosaic client by a talented and extremely enthusiastic group at the National Center for Supercomputer Applications (NCSA) at the University of Illinois in Champaign-Urbana. The Mosaic client for World Wide Web was originally developed for X-Windows under Unix, with subsequent versions released for both the Macintosh and PC platforms.

The Mosaic client software added a few new key features to the World Wide Web: the ability to display embedded images within documents, enabling authors to greatly enhance the aesthetics of their documents; the ability to incorporate links to simple multimedia items such as short movie and sound clips; and the ability to display forms. Forms greatly enhanced the original search mechanism built into WWW by allowing documents to contain fields that the user could fill in, or select from a list of choices, before clicking on a link to request further information. The introduction of forms to the WWW opened a new arena of applications in which the World Wide Web acts not only as a way of viewing static documents, but also as a way of interacting with the information in a simple but flexible manner, enabling the design of Web-based graphical interfaces to databases and similar applications.

During 1993 the usage of WWW began to grow exponentially. As new people discovered the Web they often became information providers themselves, and as more information became available new users were attracted to the Web. The graph on this page shows the growth in World Wide Web (or more accurately HTTP) traffic over the National Science Foundation backbone since early 1993, in comparison to Gopher and FTP traffic during the same period (FTP—file-transfer protocol—was one of the earliest protocols developed for the Internet, and is still the most widely used for transferring large files). While the growth in WWW traffic is enormous, it is worth noting that it is still not the dominant protocol; in fact, FTP, e-mail and NNTP (Network News transfer protocol) traffic are all substantially larger.

Owing to the distributed management of the Internet and the World Wide Web, it is very difficult to obtain hard numbers about the size of the Web or the number of users. (The number of users on the Internet, often estimated to be in the tens of millions, is itself a contentious issue, with some estimates claiming this number to be an overestimate by perhaps as much as an order of magnitude.) One illustration of the size of the Web came in early 1994 when a server was set up to provide information and up-to-the-minute results from the Winter Olympics being held in Lillehammer, Norway. The implementation of the server wasn't started until the day before the Olympics were scheduled to start, but two weeks later the server (together with a hastily arranged mirror server in the United States) had been accessed 1.3 million times, by users on somewhere between 20,000 and 30,000 different computers in 42 countries.

NCSA now estimates that more than a million copies of the Mosaic software have been taken from their distribution site, and approximate counts of the number of HTTP servers indicates there are more than 3000 servers currently operating (Stanford University alone has over 40 HTTP servers, not including one for the Stanford Shopping Center!).

HISTORY OF THE WORLD WIDE WEB

As the size of the Web has increased, so has the interest in the WWW from outside the academic community. One of the first companies to take an active interest in the World Wide Web was the publisher O'Reilly and Associates. For over a year they have provided an online service, the Global Network Navigator, using the World Wide Web. This includes regularly published articles about developments in the Internet, the "Whole Internet Catalog," an index of information available on the Web, a travel section, business section, and even daily online comics and advertising, all illustrated with professionally designed icons.

The Global Network Navigator is now only one of many examples of commercial publishers making information available on the Web, including a number of print magazines and newspapers which are available partially or in their entirety on the Web.

Another interesting example of commercial use of the World Wide Web is the CommerceNet organization. This organization, based in northern California and funded by a consortium of large high technology companies with matching funds of $6 million from the U.S. government's Technology Reinvestment Project, aims to actively encourage the development of commerce on the Internet using WWW as one of its primary enabling technologies. CommerceNet aims to encourage companies to do business on the Internet by making catalogs available and accepting electronic orders, and also by encouraging electronic collaboration between companies.

One specific way that CommerceNet is enhancing WWW is by the proposed introduction of a "secure-HTTP," which would enable encrypted transactions between clients and servers. This would ensure privacy, but perhaps more interestingly would also enable the use of digital signatures, effectively ensuring that when you fill in an order form on the Internet and submit it, it really goes to the company you believe you are ordering from (and only them), and that they know when they receive the order that it really came from you (and can prove it at a later date if necessary). This mechanism also begins to address a problem of great interest to commercial publishers—that of billing for information accessed through the Web. CommerceNet has ambitious plans to incorporate thousands of member companies in the first year or two, primarily in Northern California, but eventually to expand towards the much broader horizons of the Internet.

USES OF WORLD WIDE WEB IN HIGH ENERGY PHYSICS

While the Web has spread far from its original HEP roots, it remains an extremely useful tool for disseminating information within the widely distributed international high energy physics community. One example of the use of World Wide Web within HEP is the access provided to the SPIRES databases at SLAC, a set of databases covering a wide range of topics of relevance to HEP such as experiments, institutes, publications, and particle data.

March 1989
First proposal written at CERN by Tim Berners-Lee.

October 1990
Tim Berners-Lee and Robert Cailliau submit revised proposal at CERN.

November 1990
First prototype developed at CERN for the NeXT.

March 1991
Prototype linemode browser available at CERN.

January 1991
First HTTP servers outside of CERN set up including servers at SLAC and NIKHEF.

July 1992
Viola browser for X-windows developed by P. Wei at Berkeley.

November 1992
Midas browser (developed at SLAC) available for X-windows.

January 1993
Around 50 known HTTP servers.

August 1993
O'Reilly hosts first WWW Wizards Workshop in Cambridge, Mass. Approximately 40 attend.

February 1993
NCSA releases first alpha version of "Mosaic for X."

September 1993
NCSA releases working versions of Mosaic browser for X-windows, PC/Windows and Macintosh platforms.

October 1993
Over 500 known HTTP servers.

December 1993
John Markov writes a page and a half on WWW and Mosaic in the New York *Times* business section. *Guardian* (UK) publishes a page on WWW.

May 1994
First International WWW Conference, CERN, Geneva, Switzerland. Approximately 400 attend.

June 1994
Over 1500 registered HTTP servers.

July 1994
MIT/CERN agreement to start WWW Organization.

October 1994
Second International WWW Conference, Chicago, Illinois, with over 1500 attendees.

The largest of the SPIRES databases is the HEP preprints database, containing over 300,000 entries. In 1990 the only way to access the SPIRES databases was by logging in to the IBM/VM system at SLAC where the database resides, or by using the QSPIRES interface which could work only from remote BITNET nodes. In either case to access information you had to have at least a rudimentary knowledge of the somewhat esoteric SPIRES query language.

Since 1990, the introduction of the World Wide Web, coupled with the widespread adoption of Bulletin Boards as the primary means of distributing computer-readable versions of HEP preprints, has revolutionized the ease of access and usefulness of the information in the SPIRES databases.

The SPIRES WWW server was one of the very first WWW servers set up outside of CERN and one of the first to illustrate the power of interfacing WWW to an existing database, a task greatly simplified by WWW's distributed client-server design. Using this interface it is now possible to look up papers within the database without any knowledge of the SPIRES query language, using simple fill-out forms (for SPIRES aficionados it is possible to use the SPIRES query language through the Web too). Access to more advanced features of SPIRES, such as obtaining citation indexes, can also be performed by clicking on hypertext links. Since the access to the database is through WWW it can be viewed from anywhere on the Internet.

In addition, by linking the entries in the SPIRES databases to the computer-readable papers submitted to electronic Bulletin Boards at Los Alamos and elsewhere, it is possible to follow hypertext links from the database search results to access either the abstract of a particular paper, or the full text of the paper, which can then be viewed online or sent to a nearby printer.

The WWW interface to SPIRES has now been extended to cover other databases including experiments in HEP, conferences, software, institutions, and information from the Lawrence Berkeley Laboratory Particle Data Group. There are now over 9000 publications available with full text, and more than 40,000 accesses per week to the SPIRES databases through WWW.

Another area in which WWW is ideally suited to HEP is in providing communication within large collaborations whose members are now commonly spread around the world. Most HEP experiments and laboratories today maintain Web documents that describe both their mission and results, aimed at readers from outside the HEP field, as well as detailed information about the experiment designed to keep collaborators up-to-date with data-taking, analysis and software changes.

In addition large HEP collaborations provide an ideal environment for trying the more interactive features of WWW available now, as well as those to be introduced in the future. An example is the data monitoring system set up by the SLD collaboration at SLAC. The facility uses WWW forms to provide interactive access to databases containing up-to-date information on the performance of the detector and the event filtering and reconstruction software.

Information can be extracted from the databases and used to produce plots of relevant data as well as displays of reconstructed events. Using these tools collaborators at remote institutes can be directly involved in monitoring the performance of the experiment on a day-by-day basis.

FUTURE DEVELOPMENTS

The size of the Web has increased by several orders of magnitude over the last two years, producing a number of scaling problems. One of the most obvious is the problem of discovering what is available on the Web, or finding information on a particular topic of interest.

A number of solutions to this problem are being tried. These range from robots which roam the Web each day sniffing out new information and inserting it into large databases which can themselves be searched through the Web, to more traditional types of digital libraries, where librarians for different subject areas browse the Web, collate information, and produce indexes of their subject areas. A number of indexes are already available along these lines, or spanning the space in between these two extremes. While these are quite effective, none of them truly solves the problems of keeping up-to-date with a constantly changing Web of information and truly being able to separate the relevant from the irrelevant. This is an active area of research at many sites, together with other problems associated with scalability of the Web, such as preventing links from breaking when information moves, separating up-to-date information from obsolete information, and maintaining multiple versions of documents, perhaps in different languages.

One new area of research is the development of a new Virtual Reality Markup Language (VRML). The idea behind VRML is to emulate the success of hypertext markup language (HTML) by creating a very simple language able to represent simple virtual reality scenarios. For example, the language might be able to describe a conference room by specifying the location of tables, chairs, and doors within a room. As with HTML the idea would be to have a language which can be translated into a viewable object on almost any platform, from small PC's to high-end graphic workstations. While the amount of detail available would vary between the platforms, the essential elements of the room would be the same between the platforms. Users would be able to move between rooms, maybe by clicking on doors, would be able to see who else was in the room, and would be able to put documents from their local computer "on to the conference table" from where others could fetch the document and view it.

This type of model could be further enhanced by the ability to include active objects into HTML or VRML documents. Using this technique, already demonstrated in a number of prototypes, active objects such as spreadsheets or data plots can be embedded into documents. While older browsers would display these objects merely as static objects, newer browsers would allow the user to interact with the object, perhaps by rotating a three dimensional plot, or

World Wide Web Protocols

TECHNICALLY the World Wide Web hinges on three enabling protocols, the HyperText Markup Language (HTML) that specifies a simple markup language for describing hypertext pages, the Hypertext Transfer Protocol (HTTP) which is used by Web browsers to communicate with Web clients, and Uniform Resource Locators (URL's) which are used to specify the links between documents.

Hypertext Markup Language

The hypertext pages on the Web are all written using the hypertext markup language (HTML), a simple language consisting of a small number of tags to delineate logical constructs within the text. Unlike a procedural language such as Postscript (move 1 inch to the right, 2 inches down, and create a green WWW in 15 point bold Helvetica font), HTML deals with higher level constructs such as "headings," "lists," "images," and so on. This leaves individual browsers free to format text in the most appropriate way for their particular environment; for example, the same document can be viewed on a Mac, on a PC, or on a linemode terminal, and while the content of the document remains the same, the precise way it is displayed will vary between the different environments.

The earliest version of HTML (subsequently labeled HTML1), was deliberately kept very simple to make the task of browser developers easier. Subsequent versions of HTML will allow more advanced features. HTML2 (approximately what most browsers support today) includes the ability to embed images in documents, layout fill-in forms, and nest lists to arbitrary depths. HTML3 (currently being defined) will allow still more advanced features such as mathematical equations, tables, and figures with captions and flow-around text.

Hypertext Transfer Protocol

Although most Web browsers are able to communicate using a variety of protocols, such as FTP, Gopher and WAIS, the most common protocol in use on the Web is that designed specifically for the WWW project, the Hypertext Transfer Protocol. In order to give the fast response time needed for Hypertext applications, a very simple protocol which uses a single round trip between the client and the server is used.

In the first phase of a HTTP transfer the browser sends a request for a document to the server. Included in this request is the description of the document being requested, as well as a list of document types that the browser is capable of handling. The Multipurpose Internet Mail Extensions (MIME) standard is used to specify the document types that the browser can handle, typically a variety of video, audio, and image formats in addition to plain text and HTML. The browser is able to specify weights for each document type, in order to inform the server about the relative desirability of different document types.

In response to a query the server returns the document to the browser using one of the formats acceptable to the browser. If necessary the server can translate the document from the stored format into a format acceptable to the browser. For example the server might have an image stored in the highly compressed JPEG image format, and if a browser capable of displaying JPEG images requested the image it would be returned in this format; however, if a browser capable of displaying images only if they are in GIF format requested the same document the server would be able to translate the image and return the (larger) GIF image. This provides a way of introducing more sophisticated document formats in the future but still enabling an older or less advanced browser to access the same information.

In addition to the basic "GET" transaction described above the HTTP is also able to support a number of other transaction types, such as "POST" for sending the data for fill-out forms back to the server and "PUT" which might be used in the future to allow authors to save modified versions of documents back to the server.

Uniform Resource Locators

The final keys to the World Wide Web are the URLs which allow the hypertext documents to point to other documents located anywhere on the Web. A URL consists of three major components:

<protocol>://<node>/<location>

The first component specifies the protocol to be used to access the document, for example, HTTP, FTP, or Gopher, etc. The second component specifies the node on the network from which the document is to be obtained, and the third component specifies the location of the document on the remote machine. The third component of the URL is passed without modification by the browser to the server, and the interpretation of this component is performed by the server, so while a document's location is often specified as a Unix-like file specification, there is no requirement that this is how it is actually interpreted by the server.

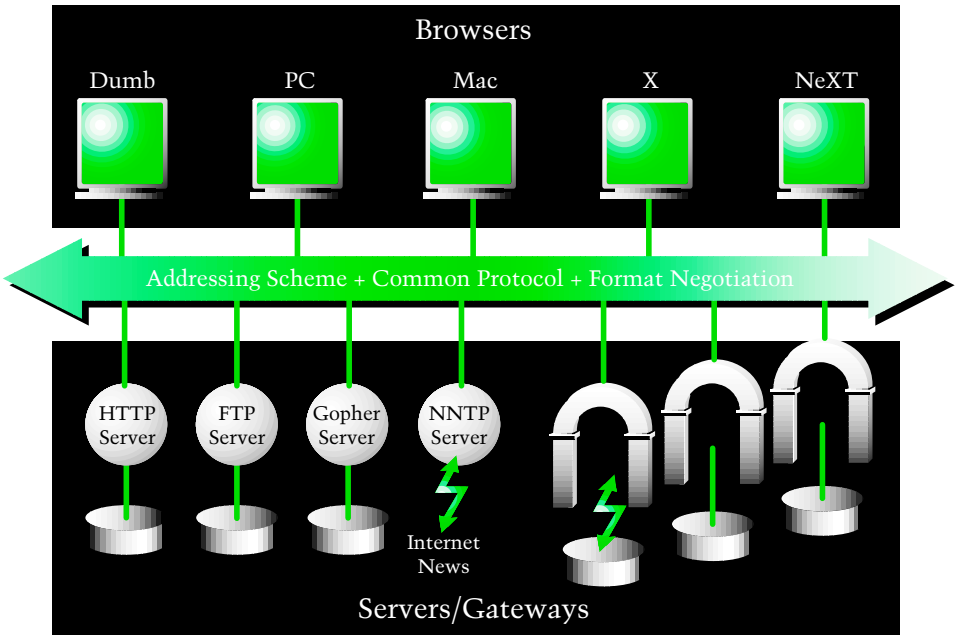

The ability of Web browsers to communicate and negotiate with remote servers allows users on a wide variety of platforms to access information from many different sources around the world.

expanding and rebinning a particular area of a data plot.

Currently the Web is viewed mainly as a tool for allowing access to a large amount of "published" information. The new features described here, together with the encryption features described earlier that will allow more sensitive data to be placed on the Web, will open up the Web to a whole new area, where it will be viewed more as a "collaborative tool" than purely an information retrieval system. Ideally it will be possible to take classes on the Web, to interact with the instructor and fellow pupils, to play chess on the Web, to browse catalogs and purchase goods, and to collaborate actively in real-time with colleagues around the world on such tasks as document preparation and data analysis.

CONCLUSION

Over the previous year the characteristics of the average Internet user have changed dramatically as many new people are introduced to the Net through services such as America Online, aimed primarily at home users. The current Web usage is likely to be insignificant in comparison to the potential for usage once the much vaulted "Information Super Highway" reaches into peoples' homes.

It is perhaps unlikely that the services eventually offered domestically on the Information Super Highway will be direct descendants of the World Wide Web, but what is clear is that WWW offers an excellent testing ground for the types of services that will eventually be commonplace. As such, the WWW may play a key role in influencing how such systems develop. At worst such a system may just become a glorified video delivery system and integrated home shopping network with a built-in method of tracking your purchases and sending you personalized junk e-mail. At its best such as system could provide truly interactive capabilities, allowing not only large corporations and publishers but also individuals and communities to publish information and interact through the network, while maintaining individual privacy. The outcome will have a major impact on the quality of life in the 21st century, influencing the way we work, play, shop, and even how we are governed.

ELECTRONIC SOURCES

THE SPIRES database and SLD information featured in this article can be accessed from the SLAC home page at:

http://www-slac.slac.stanford.edu/FIND/slac.html

The illustrations on the Web in this article show the Midas WWW browser developed at SLAC. Information on obtaining and using this browser is available from:

http://www-midas.slac.stanford.edu/midas_latest/introduction.html

Pointers to other pages mentioned in this article:

Global Network Navigator:
http://nearnet.gnn.com/gnn/GNNhome.html

CommerceNet:
http://www.commerce.net

Stanford Shopping Center:
http://netmedia.com/ims/ssc/ssc.html

What Have We Learned About Solar Neutrinos?

by JOHN N. BAHCALL

The apparent deficit of solar neutrinos may be caused by physical processes beyond the Standard Model.

THIRTY YEARS AGO Ray Davis—then working at Brookhaven and now at Pennsylvania—suggested it was practical to build an experiment to detect solar neutrinos if the event rate I calculated was correct. The proposal was based upon his experience at the Savannah River reactor trying to detect antineutrinos using a tank filled with 3,000 gallons of perchloroethylene ($C_2 Cl_4$, a common cleaning fluid), and on calculations that I had done of the event rate to be expected in a 100,000 gallon tank.

These calculations were in turn based upon nuclear physics estimates of the neutrino capture rates and solar model calculations of the neutrino fluxes. Ray was confident that he could build and successfully operate the 100,000 gallon tank, extracting the few radioactive atoms of argon produced each month due to neutrino capture by chlorine atoms ($^{37}Cl \rightarrow {}^{37}Ar$) in this huge detector. Thirty years later it is clear that he was right and the then-abundant skeptics were wrong.

At the time this chlorine experiment was proposed, the only motivation either of us presented for performing a solar neutrino experiment was to use neutrinos "to see into the interior of a star and thus directly verify the hypothesis of nuclear energy generation in stars." The hypothesis being tested was that stars like the Sun shine by fusing protons to form alpha particles, positrons, neutrinos, and thermal energy.

The original goal of demonstrating that proton fusion is the origin of sunshine has been achieved. Solar neutrinos have now been observed in four different experiments with (to usual astronomical accuracy) fluxes and energies that are in rough agreement with the expected values. The observed rates in all of the solar neutrino experiments are only about a factor of 2 or 3 less than expected (see chart on this page). Moreover, the fact that the neutrinos indeed come directly from the Sun was established by one of these experiments (Kamiokande), which showed that electrons scattered by interacting neutrinos recoil in the forward direction—away from the Sun. The characteristics of the operating solar neutrino experiments were discussed by Ken Lande in the Fall 1992 *Beam Line*; they are summarized in the table on the next page. The results of these experiments represent a triumph for the combined physics, chemistry, and astronomy communities because they bring to a successful conclusion the development (which spanned much of the twentieth century) of a theory of how ordinary stars—those like the Sun—shine.

Comparisons between the predicted fluxes of the standard solar model and the four operating solar neutrino experiments. The unit used for the three radiochemical experiments is a solar neutrino unit, or SNU, which equals one event per second per 10^{36} target atoms. Following the experimenters, the Kamiokande result is expressed in terms of a ratio to the expected event rate. Predictions shown in this figure and quoted elsewhere in this article are from the Bahcall-Pinsonneault 1992 standard solar model with helium diffusion. The observed rates are less than the expected rates for all four experiments.

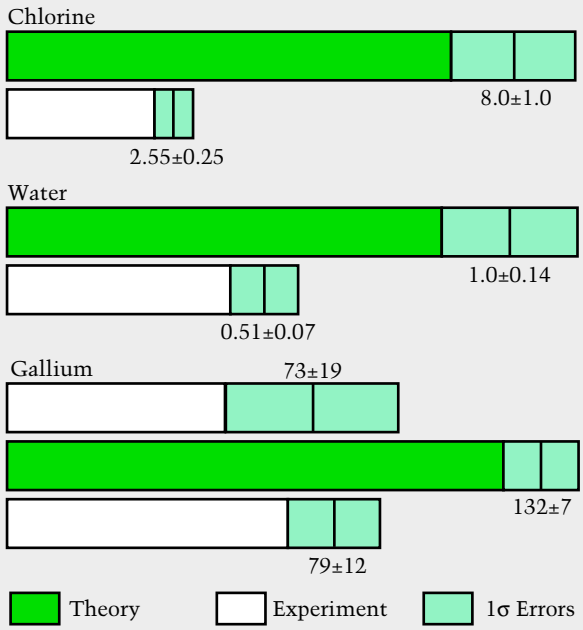

MOST OF THE CURRENT interest in solar neutrinos is focused on an application of this research that was not even discussed when the Homestake chlorine detector was proposed. Scientists have realized that they can use solar neutrinos for studying aspects of the weak interactions that are not accessible in laboratory experiments. Such searches for new physics are based upon quantitative discrepancies between the predictions for and the observations of solar neutrinos. As the experiments and the theoretical predictions have steadily improved over the past three decades, these discrepancies have resolutely refused to go away, convincing many of us who work in this field that we have been witnessing the discovery of new physics in an unexpected context.

Although thirty years ago I was a skeptic about the theory of stellar evolution and did not believe in any explanation of astronomical phenomena that required changing conventional physics, my preconceptions have since been shaken by the robustness of the theory and by the combined results of the four solar

Operating Solar Neutrino Experiments

Name	Target	Mass (tons)	Threshold (MeV)	Detector Type	Location
Homestake	^{37}Cl	615	0.86	radiochemical	Black Hills, South Dakota
Kamiokande	H_2O	680	7.5	electronic	Japanese Alps
GALLEX	^{71}Ga	30	0.2	radiochemical	Gran Sasso, Italy
SAGE	^{71}Ga	57	0.2	radiochemical	Caucasus Mtns., Russia

neutrino experiments. I now think it is most likely that we are witnessing evidence for new physics in these experiments.

Solar neutrino observations are often compared to a combined theoretical model, the standard solar model plus the Standard Model of electroweak interactions. A solar model is required to predict how many—and with what energies—neutrinos are produced in the Sun's interior. The observed luminosity of the sun (due to the same nuclear processes that produce solar neutrinos) and the other observational constraints on the solar model (including the Sun's known age, mass, chemical composition, and its many precisely measured seismological frequencies) limit the calculated fluxes to fairly narrow regions, at least by astrophysical standards (see box on next page).

The standard electroweak model—or some modification of the Standard Model—is required to determine what happens to neutrinos as they pass through the Sun and interplanetary space on their way from the solar interior to earthbound detectors. The observed discrepancies might occur if neutrinos decay in transit, or if they change from one species to another before reaching the detectors. The three radiochemical detectors register only electron neutrinos, while the only electronic detector (Kamiokande) registers both electron neutrinos and (with much reduced sensitivity) muon or tau neutrinos.

Do electron neutrinos change their flavor, or "oscillate," into hard-to-detect muon or tau neutrinos during their journey from the interior of the Sun to the Earth? The simplest version of the standard electroweak model answers "No." Neutrinos have zero masses in the Standard Model, and lepton flavor does not change. However, solar neutrinos can reveal physical processes not yet discovered in the laboratory because, for certain processes, these experiments are 10^{11} times more sensitive than terrestrial neutrino experiments. Their increased sensitivity is due largely to the fact that the elapsed time in the rest frame of a (finite-mass) neutrino is proportional to the ratio of the target–detector separation to the neutrino energy; this ratio is much larger for neutrinos originating in the Sun. Moreover, solar neutrinos traverse a far greater amount of matter than their laboratory counterparts.

THE FIRST, and for two decades the only, solar neutrino experiment uses a chlorine detector to observe electron-type neutrinos via the reaction $\nu_e + {}^{37}\mathrm{Cl} \rightarrow e^- + {}^{37}\mathrm{Ar}$. The ^{37}Ar atoms produced by this neutrino capture process are extracted chemically from the 615 tons of perchloroethylene in which they were created; they are then counted using their characteristic radioactivity in small, gaseous proportional counters. The threshold energy is 0.8 MeV, which means (see figure on the next page) that this experiment is sensitive to the rare

high-energy ^{8}B neutrinos, as well as to the lower energy *pep* and ^{7}Be neutrinos formed by electron capture on two fusing protons and on ^{7}Be nuclei. Like all solar neutrino experiments, the chlorine experiment is performed deep underground (in the Homestake gold mine, in Lead, South Dakota) in order to avoid cosmic-ray induced events that might be confused with true neutrino events.

In the Kamiokande experiment, which is carried out in Kamioka mine in the Japanese Alps, neutrino-electron scattering, $\nu + e \rightarrow \nu' + e'$, occurs inside the fiducial mass of 680 tons of ultrapure water. The scattered electrons are detected by the Cerenkov light that they produce while speeding through the water. The fact that the neutrinos are coming directly from the Sun was established by this experiment, which showed that the electrons were scattered in the forward direction, relative to the Sun. Only the rare, high-energy ^{8}B solar neutrinos can be detected in the Kamiokande experiment, for which the detection threshold is at least 7.5 MeV. The probability of detecting muon or tau neutrinos by their scattering of atomic electrons is only about 17 percent of the equivalent probability of detecting electron neutrinos at the energies for which Kamiokande is sensitive.

Two gallium experiments are in progress, GALLEX (located in the Gran Sasso underground laboratory about an hour's drive from Rome) and SAGE (in an underground chamber excavated beneath the Andyrchi mountains in the North Caucasus region of Russia). Performed by two international collaborations, these experiments provided the first observational information about the low-energy neutrinos from the basic proton-proton fusion reaction. Both experiments use neutrino absorption by gallium atoms to produce germanium, $\nu_e + {}^{71}\mathrm{Ga} \rightarrow e^- + {}^{71}\mathrm{Ge}$, which has a threshold of only 0.2 MeV for neutrino detection. Such a low threshold allows the detection of the low-energy *pp* neutrinos, for which the flux is known to an accuracy of

SOLAR NEUTRINO FLUXES

The spectrum of solar neutrinos that is predicted by the standard solar model is shown in the graph below. The basic low-energy neutrino fluxes, from *pp* and *pep* neutrinos, are most closely related to the total solar luminosity and are calculated to an estimated accuracy of about 1 percent. These reactions initiate the nuclear fusion chain in the Sun and produce neutrinos with a maximum energy of 0.4 MeV (*pp* neutrinos) or an energy of 1.4 MeV (*pep* neutrinos). Electron-capture by ^{7}Be ions produces the next most abundant source of neutrinos, a 0.86 MeV neutrino line, whose flux has an estimated theoretical error of 6 percent. Neutrinos from the beta decay of ^{8}B can have energies as high as 14 MeV; they are rare and their flux is calculated to an estimated accuracy of only 15 percent.

pp: $p + p \rightarrow {}^2H + e^+ + \nu_e$

pep: $p + e^- + p \rightarrow {}^2H + \nu_e$

^{7}Be: $^7Be + e^- \rightarrow {}^7Li + \nu_e$

^{8}B: $^8B \rightarrow {}^8Be + e^+ + \nu_e$

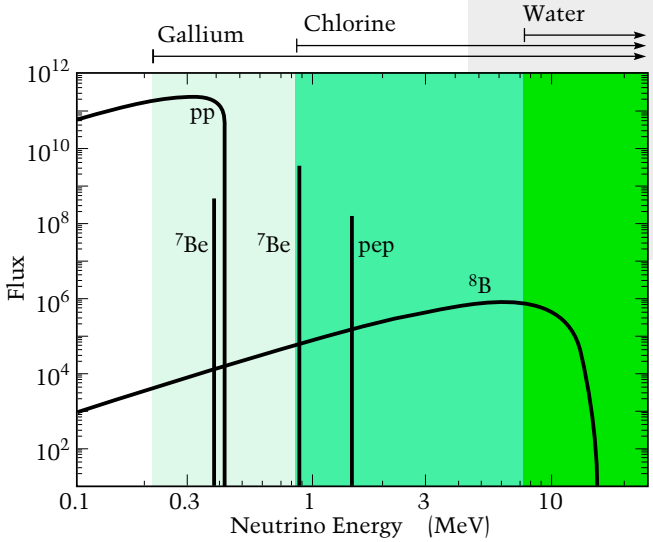

The energy spectrum of neutrinos from the pp chain of interactions in the Sun, as predicted by the standard solar model. Neutrino fluxes from continuum sources (such as pp and ^{8}B) are given in the units of counts per cm^2 per second per MeV. The line fluxes (pep and ^{7}Be) are given in neutrinos per cm^2 per second. The pp chain is responsible for more than 98 percent of the energy generation in the standard solar model. Neutrinos produced in the carbon-nitrogen-oxygen CNO chain are not important energetically and are difficult to detect experimentally. The arrows at the top of the figure indicate the energy thresholds for the ongoing neutrino experiments.

LANL (Thomas J. Bowles)

Containers of gallium in the SAGE experiment, which detects solar neutrinos down to a threshold energy of 0.2 MeV

1 percent. The GALLEX and the SAGE experiments use radiochemical procedures to extract and count a small number of atoms from a large detector, similar to what is done in the Homestake chlorine experiment.

All four solar neutrino experiments yield fluxes significantly less than predicted and well outside the combined errors (see chart on page 11). One fact is immediately apparent: the disagreement between theory and experiment seems to depend upon the threshold for neutrino detection, being a factor of about 3.1 for the Homestake chlorine experiment (0.8 MeV threshold) and only 2.0 for the Kamiokande water experiment (7.5 MeV threshold). These two experiments are primarily sensitive to the same neutrino source, the rare, high-energy ^{8}B solar neutrinos; their sensitivity to threshold energy suggests that some physical process, in addition to the familiar nuclear beta-decay, changes the energy spectrum of these neutrinos before they reach the detectors.

THE MARKED discrepancies between predicted and measured neutrino fluxes is known as the "solar neutrino problem." It cannot be "solved" by making plausible changes in the standard solar model or by postulating that only one or two solar neutrino experiments are incorrect. As I argue in the boxes on pages 15 and 16, the least radical solutions are: at least three of the four experiments are wrong, or something unexpected happens to neutrinos after they are created in the solar interior. The latter solution requires a slight but important generalization of the simplest version of the standard electroweak theory.

I use only the published results of the four ongoing solar neutrino experiments and the most robustly predicted neutrino fluxes from published standard solar models. As a measure of the uncertainty in the predictions, I use the total range of the calculated neutrino fluxes from the 11 recently-published solar model calculations carried out by different research groups using independent stellar evolution codes and employing a wide range of possible input parameters and approximations to the stellar physics.

Some particle physicists have expressed skepticism about the solar neutrino problem because the calculated flux of high-energy neutrinos from ^{8}B beta-decay depends strongly upon the central temperature of the Sun. A related concern is being discussed among nuclear physicists, who are using recent experiments and new calculations to determine whether the 9 percent uncertainty estimated by CalTech physicists for the production cross section of ^{8}B nuclei in the Sun is indeed valid. The calculated flux of ^{8}B neutrinos is proportional to this cross section.

I personally believe that the previously estimated nuclear physics uncertainties are reasonable. But for the purposes of the present argument—and to allay skepticism—I

The Chlorine-Water Problem

THE HOMESTAKE AND THE KAMIOKANDE solar neutrino experiments are not consistent with each other unless some physical process—not included in standard electroweak theory—affects the energy spectrum of ^{8}B neutrinos. The argument leading to this conclusion goes as follows:

The most recent result of the Kamiokande experiment for the rare ^{8}B neutrinos is

$$\text{Flux}(^8\text{B}) = (2.89 \pm 0.41) \times 10^6 \text{ cm}^{-2}\text{s}^{-1}, \quad (1)$$

where I have combined quadratically (both here and below) the statistical and systematic errors. I have shown elsewhere that if standard electroweak theory is correct, then the shape of the energy spectrum from ^{8}B solar neutrinos must be the same (to 1 part in 10^5) as the shape determined by laboratory experiments. The absorption cross section is known accurately for ^{8}B neutrinos with a standard energy spectrum incident on a ^{37}Cl nucleus. Therefore, if standard electroweak theory is correct, the capture rate in the Homestake chlorine experiment from the ^{8}B neutrino flux observed in the Kamiokande experiment should be

$$\text{Rate in Cl } (^8\text{B}) = (3.21 \pm 0.46) \text{ SNU}, \quad (2)$$

where 1 SNU = 1 neutrino capture per 10^{36} target atoms per second. But the observed rate in the chlorine experiment from *all* neutrino sources is

$$\text{Obs Rate in Cl} = (2.55 \pm 0.25) \text{ SNU}. \quad (3)$$

Subtracting the rate due to ^{8}B neutrinos as determined by the Kamiokande experiment (2) from the rate due to all neutrino sources (3), we find that the best estimate for the capture rate in the chlorine experiment from all sources *except* ^{8}B neutrinos, assuming standard electroweak theory to be correct, is

$$\text{Obs Rate in Cl}(pep + {}^7\text{Be} + \text{CNO}) = -0.66 \pm 0.52 \text{ SNU}, \quad (4)$$

where CNO represents the sum of all neutrino-producing reactions in the CNO cycle. This negative value for the sum of the capture rates from three different neutrino sources is the simplest expression of the "solar neutrino problem." It is independent of the solar model used.

Although the best estimate for the residual capture rate for *pep,* ^{7}Be and CNO solar neutrinos is negative, the physical capture rate for any set of neutrino fluxes has to be positive definite. Adopting the conservative procedure used by the Particle Data Group in analogous discussions (for example, upper limits to neutrino masses), we find:

$$\text{Rate in Cl}(pep + {}^7\text{Be} + \text{CNO}) \leq 0.68 \text{ SNU (95\% conf.)}. \quad (5)$$

We can refine this result by utilizing the fact that the flux of neutrinos from the *pep* reaction is directly related to the basic *pp* reaction, which is the initiating fusion reaction that produces nearly all of the solar luminosity in standard solar models. The total spread in the calculated capture rates for *pep* neutrinos for the 11 recently published standard solar models (calculated with different codes and input parameters) is 0.22 ± 0.01 SNU. Subtracting this accurately-known *pep* flux from the the upper limit for the three neutrino sources shown in (5), we obtain:

$$\text{Rate in Cl}({}^7\text{Be} + \text{CNO}) \leq 0.46 \text{ SNU (95\% conf.)}. \quad (6)$$

The ^{7}Be neutrino flux is predicted with reasonable accuracy; the results from the 11 different standard solar models yield the value

$$\text{SSM Rate in Cl}({}^7\text{Be}) = 1.1 \pm 0.1 \text{ SNU}. \quad (7)$$

Thus the upper limit on the sum of the capture rates from ^{7}Be and CNO neutrinos is significantly less than the lowest value predicted for ^{7}Be neutrinos alone, by any of the 11 recent standard solar models. I did not subtract the CNO neutrino capture rate from the sum of the two rates because the conflict between the measurements and the standard models (solar and electroweak) is apparent without this additional step and because the estimated rate from CNO neutrinos, 0.4 ± 0.08 SNU, is more uncertain than for the other neutrino fluxes being considered.

The Gallium Problem

THE GALLEX AND THE SAGE gallium solar neutrino experiments have reported consistent neutrino capture rates (respectively, 79±12 SNU and 73±19 SNU). From the weighted average of their results, the best estimate for the gallium rate is

$$\text{Obs Rate in Ga} = 77 \pm 10 \text{ SNU}. \quad (8)$$

All standard solar models yield essentially the same predicted event rate from *pp* and *pep* neutrinos, 74 ± 1 snu. Subtracting this rate from the total observed rate, one finds that the residual rate from ^{7}Be and ^{8}B solar neutrinos in gallium is small,

$$\text{Rate in Ga}(^{7}\text{Be} + {}^{8}\text{B}) = 3 \pm 10 \text{ SNU}, \quad (9)$$

which implies that the upper limit on this rate is

$$\text{Rate in Ga}(^{7}\text{Be} + {}^{8}\text{B}) \leq 22 \text{ SNU (95\% conf.)}. \quad (10)$$

This combined ^{7}Be and ^{8}B rate is less than the predictions from ^{7}Be neutrinos alone for all 11 recently-published standard solar models.

Moreover, one should take account of the ^{8}B neutrino flux that is observed in the Kamiokande experiment, which in the gallium experiments translates to

$$\text{Rate in Ga}(^{8}\text{B}) = 7.0^{+7}_{-3.5} \text{ SNU}, \quad (11)$$

where the quoted errors are dominated by uncertainties in the calculated neutrino absorption cross sections and I have assumed that the shape of the energy spectrum of ^{8}B solar neutrinos is the *same* as measured in the laboratory. Subtracting this rate for ^{8}B neutrinos from the combined rate of ^{7}Be and ^{8}B neutrinos, one again finds that the best-estimate flux for ^{7}Be neutrinos is negative.

$$\text{Rate in Ga}(^{7}\text{Be}) = -4^{+11}_{-12} \text{ SNU}. \quad (12)$$

Following the same statistical procedure as described earlier, one can set a conservative upper limit on the ^{7}Be neutrino flux using the gallium and the Kamiokande measurements:

$$\text{Rate in Ga}(^{7}\text{Be}) \leq 19 \text{ SNU (95\% conf.)}. \quad (13)$$

The predicted rate given by the 11 standard solar models is

$$\text{SSM Rate in Ga}(^{7}\text{Be}) = 34 \pm 4 \text{ SNU}. \quad (14)$$

The discrepancy between these two equations is a quantitative expression of the gallium solar neutrino problem.

The present results for the gallium experiments are close to being in conflict with a model-independent, unrealistically conservative upper limit on the counting rate. This minimum counting rate of 80 SNU is calculated assuming only that the Standard Model is correct and that the Sun is currently producing nuclear fusion energy at the same rate at which it is losing photon energy from the surface. To reach the lower limit of 80 SNU in a solar model, one must set equal to zero the rates of all nuclear reactions that produce ^{7}Be in the sun. We know that this limit cannot be satisfied in practice because we observe high energy ^{8}B neutrinos and ^{8}B is produced by proton capture on ^{7}Be—and because the cross section for creating ^{7}Be has been measured in the laboratory to be competitive with the other solar fusion rates.

will assume that *all* of the published laboratory measurements and theoretical nuclear physics calculations are wrong and that the cross section for ^{8}B production in the Sun has somehow been adjusted to yield the flux measured for these high-energy neutrinos in the Kamiokande experiment. This implies that the laboratory nuclear physics measurements are in error by a factor of 2, not by 9 percent. Since I adopt the ^{8}B neutrino flux measured in the Kamiokande experiment, the ^{8}B flux used in the following discussion is independent of any solar-model uncertainties (including the sensitive temperature dependence). This procedure removes a principal reason for skepticism. Even this extreme assumption does not avoid the necessity for new physics, as we shall see.

The argument described here, most of which was developed in a slightly different form by Hans Bethe and myself in 1990, avoids all uncertainties associated with the solar model calculation of the ^{8}B flux. We pointed out that taking the measured rate for ^{8}B neutrinos from the Kamiokande experiment implies an ^{8}B event rate in the Homestake experiment that is slightly in excess of the total measured rate from *all* neutrino sources. In other words, a partial rate exceeds the total rate, which makes no sense unless something happens to the lower-energy part of the ^{8}B electron neutrino flux—that part of the flux which is visible in the Homestake chlorine experiment but not in the Kamiokande water experiment. This direct comparison of two experiments—independent of any solar model considerations—suggests

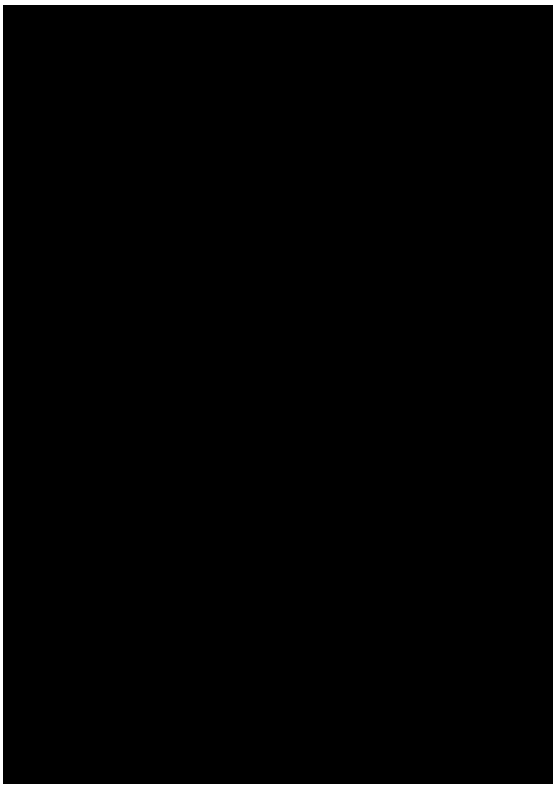

GALLEX collaboration

One of the large containers of gallium used in the GALLEX solar neutrino experiment, which is located in the Gran Sasso underground laboratory in Italy.

that a new physical process causes the discrepancy between the experiments.

There are actually *two* solar neutrino problems: the chlorine-water problem and the gallium problem. In the box on page 15, I show why the measured rates of the chlorine and the water experiments are inconsistent with each other, unless some new physical process—not included in the standard electroweak model—changes the shape of the energy spectrum of ^{8}B neutrinos in transit to the detector. In the box on page 16 I argue that the gallium experiments are inconsistent with robust predictions of the standard solar model.

Let me assume for purpose of discussion that a correct solar neutrino experiment must yield a rate for the ^{7}Be neutrino flux that is consistent (at the 95% confidence level) with nothing happening to solar neutrinos after they are created (i.e., the standard electroweak theory) and with the value of the ^{7}Be neutrino flux that is predicted by the standard solar model. If these assumptions are both correct, then at least three of the four operating solar neutrino experiments must be wrong. Either the Homestake or the Kamiokande experiment must be wrong in order to avoid the chlorine-water problem (see box on page 15) and both the GALLEX and SAGE experiments must be wrong in order to avoid the gallium problem (see box on page 16).

THE TWO MOST POPULAR mechanisms for explaining the solar neutrino problem via new physics are vacuum neutrino oscillations, first discussed in this connection by Vladimir Gribov and Bruno Pontecorvo in an epochal paper, and matter-enhanced neutrino oscillations, the MSW effect, a beautiful idea discovered by Lincoln Wolfenstein and also by Stanislav Mikheyev and Alexei Smirnov. Other solutions have been proposed for the solar neutrino problem that involve new weak interaction physics, such as neutrino decay, rotation of the neutrino magnetic moment, and matter-enhanced magnetic moment transitions.

If new physics is required, then the MSW effect, which provides a natural extension of the simplest version of standard electroweak theory, is in my view the most likely candidate. According to this explanation, electron neutrinos are transformed into muon or tau neutrinos as a result of their interaction with electrons in the Sun. The MSW effect only occurs if neutrinos have an "identity crisis"—i. e., the neutrinos produced in nuclear beta decay are mostly electron neutrinos but have a non-vanishing probability (described by a mixing angle θ) of being either a muon or a tau neutrino. Non-zero neutrino masses are required for this effect to occur in a plausible manner, but the masses and mixing angles indicated by experiment are within the range expected on the basis of grand unified theories. If the MSW effect is the explanation of the solar neutrino problem, then the Homestake, Kamiokande and the two gallium experimental results can all be explained (see graph) if at least one neutrino coupled to the electron neutrino has a mass m and a mixing angle θ that satisfy: $m^2 \sim 10^{-5}$ eV^2 and $\sin^2 2\theta \sim 10^{-2}$ or $m^2 \sim 10^{-5}$ eV^2 and $\sin^2 2\theta \sim 0.6$.

The regions in mass and mixing angle space that are consistent with all four solar neutrino experiments. This figure, prepared by Naoya Hata and Paul Langacker, shows two possible solutions of the solar neutrino problem that make use of the MSW effect. Both solutions correspond to some neutrinos having a mass of order 0.003 eV.

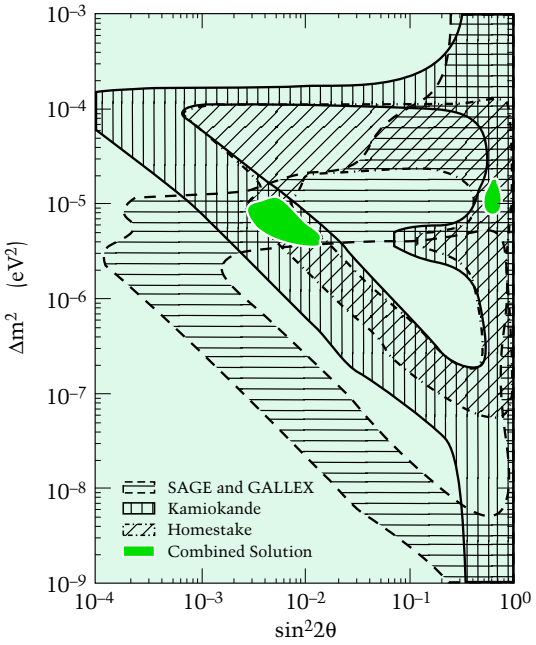

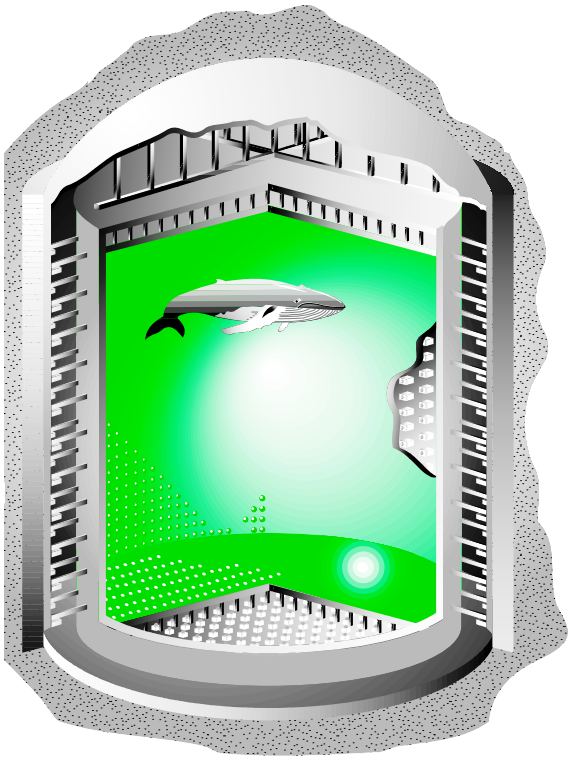

Artist's conception of the Super Kamiokande detector now under construction in the Japanese Alps. This huge tank, containing 50,000 tons of ultrapure water viewed by over 11,000 phototubes, will be used to search for proton decay and to detect solar neutrinos, among other goals. (The 60 foot humpback whale is shown only for size comparison and is not a part of this experiment!)

New solar neutrino experiments now under construction will soon test the proposition that new physics is required, independent of uncertainties due to solar models. The first of these experiments (the Sudbury Neutrino Observatory, or SNO, and Super Kamiokande) are expected to become operational in 1996 and to increase the counting rates by two orders of magnitudes over those observed in the four pioneering solar neutrino experiments. (see "New Solar Neutrino Detectors," by Ken Lande, Fall 1992 *Beam Line*, page 9, for a brief discussion of these experiments). These two experiments and another called ICARUS (being developed at CERN) can determine the shape of the ^{8}B solar neutrino energy spectrum and whether or not electron neutrinos have oscillated into some other kind of neutrino. And a liquid scintillator detector named BOREXINO will provide the first direct measurement of the crucial flux of ^{7}Be neutrinos.

In the meantime, scientists and engineers can take great satisfaction that thirty years of their collective efforts have provided direct experimental confirmation, in the form of measured neutrinos, of the theory of how ordinary stars shine. Physicists and chemists have collaborated to perform extraordinarily sensitive experiments that measure accurately the event rates produced by solar neutrinos. Astrophysicists have successively refined their calculations of solar models until they are in agreement with a wealth of detailed (non-neutrino) solar observations. Their theoretical calculations of the neutrino interaction rates have been steadily improved with the help of new experimental data. Finally, theoretical physicists have invented new physical processes that extend the standard electroweak model in plausible ways and which, in addition to explaining the operating experiments, make testable predictions for the next round of solar neutrino experiments. Important limits on the magnitudes of possible non-standard neutrino interactions have already been established by the existing experiments. After the new experiments begin operating, we should finally learn whether or not we have stumbled by accident upon new particle physics while trying to test the theory of how the Sun shines.

Biological Applications of SYNCHROTRON RADIATION

by ROBERT A. SCOTT

Intense X-rays from synchrotrons are used to determine biological structure at every level of spatial resolution.

ANYONE LOOKING for the strategic importance of high-energy physics research to the nation need look no further than the applications spawned by the harnessing of synchrotron radiation as a spinoff from particle storage rings. Synchrotron radiation (SR) light sources have given rise to technological innovations in a number of fields including chemistry, materials research, geology, and biology.

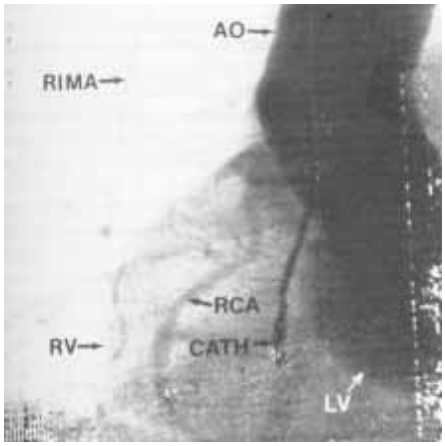

An example of a coronary angiogram recorded at the Stanford Synchrotron Radiation Laboratory in a 64 year old man. Visible are the aorta (AO), the right internal mammary artery (RIMA), the right coronary artery (RCA), and the left ventricle (LV). This image was recorded after the contrast agent had cleared the right heart so the right ventricle (RV) is virtually transparent [from Nucl. Instr. Meth. A266, *252–259 (1988)].*

It is ironic that the intense ionizing X-rays provided by SR that can do so much damage to biological specimens (e.g., human tissue) have contributed to a revolution in our methods of investigation of a number of biological systems and processes. To date, this revolution can be described in terms of improvements in our ability to determine the structure of biological materials at every level of spatial resolution, from macroscopic imaging to atomic-level structural detail. As the next generation of SR sources turn on during the next few years, a second revolution will occur in the enhanced temporal resolution of these techniques; tantalizing glimpses of the power of these new time-resolved methods are already available today. In this article, I review these SR-based techniques of structural biology and give examples of how they have been applied to problems of biomedical and biotechnological importance.

Most of the studies discussed here use photons in the X-ray region of the synchrotron radiation spectrum. The major advantage that X-rays have over photons in other regions of the electromagnetic spectrum is that they possess wavelengths that are on the order of molecular dimensions [in the Ångstrom (Å), 10^{-10} m, range]. Thus it is a special property of X-rays that their interaction with matter is directly sensitive to structure at the molecular level. Most of the biological applications dealing with this level of structural detail take advantage of this property. However, X-rays can also be used in spectroscopy, that is, measurement of the wavelength-dependent absorption or scattering of X-rays by matter. In spectroscopy-based applications, the X-rays are used to excite electrons within atoms and molecules, and these excitations are wavelength dependent. If a biological specimen absorbs strongly X-rays of one wavelength, but does not absorb X-rays of another wavelength, then comparing the two-dimensional absorption patterns of a specimen at the two different wavelengths gives rise to *contrast* which can be used to image that specimen. This allows access to structure at a macroscopic (millimeter, 10^{-3} m) or microscopic (submicrometer, 10^{-6} m) level. Let's start by looking at these latter imaging techniques and then work our way down to the atomic level.

X-RAY IMAGING TECHNIQUES

Coronary Angiography

A premiere example of the application of synchrotron radiation to the medical field is the development of non-invasive coronary angiography [see "Imaging the Heart Using Synchrotron Radiation," by George A. Brown, Fall/Winter 1993 *Beam Line* page 22]. Most patients today being tested for arterial restriction or blockage are treated by invasive angiography, which involves catheter-based arterial injection of contrast agent, an inherently dangerous procedure. SR-based coronary angiography takes advantage of the tunability of SR by using a contrast agent containing iodine and measuring images above and below the iodine K absorption edge at 33.16 keV. (K edges are sharp discontinuities in the X-ray absorption coefficient at the energy required to photodissociate an electron bound

in the 1*s* orbital of atoms of a given element. In this case, iodine-containing materials are nearly transparent to X-rays with energies below 33.16 keV, but nearly opaque to X-rays with energies above 33.16 keV.) This yields high-contrast images after subtraction of the image obtained with X-rays below the iodine edge from the image obtained above the iodine edge. The high contrast allows the contrast agent to be delivered intravenously rather than by arterial injection, eliminating much of the risk in the procedure. The standard procedure uses a broad SR beam that is intercepted by a horizontal linear position-sensitive detector behind the patient. The patient is then scanned vertically so that the SR beam passes through all sections of the heart. A fast shutter is used to control the irradiation time at each vertical position. This results in line-scan images much like the images seen on a television. Digital subtraction and image processing yield high-quality two-dimensional coronary images. This field has advanced from the inception of the idea and first experiments at Stanford Synchrotron Radiation Laboratory (SSRL) in 1979 to the establishment of a clinical facility at the National Synchrotron Light Source at Brookhaven called the Synchrotron Medical Research Facility. Recent advances in SR-based angiography include attempts to develop it into a real-time imaging procedure and the extension from two- to three-dimensional imaging. In the latter development, two SR beams strike the patient at slightly different angles, generating stereo-pair images that can be viewed as three-dimensional objects.

X-ray Computed Tomography

True three-dimensional medical imaging is also being pursued in projects at several SR sources to develop X-ray computed tomography. Eventually, this technique is expected to yield higher resolution images than the conventional positron emission tomography (PET). A monochromatic horizontal X-ray fan beam is used to give a projection image of a subject that is rotated about a vertical axis, and a slice of the three-dimensional image is reconstructed. Stepping the subject vertically allows for other slices to be acquired, then stacked into a three-dimensional image. Use of X-rays of various wavelengths and digital subtraction allows imaging of the distribution of materials containing different elements, a feat that is impossible with PET. An example of *in vivo* imaging of bone structure is shown in the figure. This experiment was performed on live anesthetized rats that had been ovariectomized to investigate a correlation between estrogen depletion and bone density that may be responsible for the high level of osteoporosis in older women.

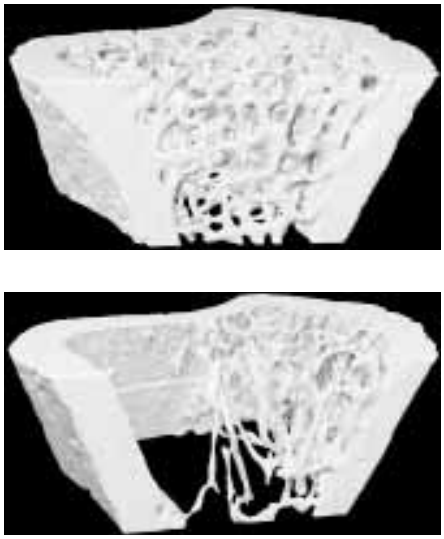

Effect of estrogen depletion on bone volume. The top image shows a slice of the proximal tibia of a 6-month-old rat, and the bottom image shows the same slice 5 weeks after ovariectomy. An overall 60% loss in bone volume has resulted from the estrogen depletion induced by ovariectomy, and disconnected bone fragments are visible. These studies are designed to detail the effects of estrogen depletion in osteoporosis in older women. [For more information on the X-ray tomographic microscope used for this study, see Annu. Rev. Mater. Sci. 22, 121-152 (1992)].

Soft X-ray Microscopy

Both angiography and tomography can image structures at about 10^{-3}–10^{-5} m resolution. For resolution in the 10^{-6}–10^{-8} m range, X-ray microscopy has been shown to be the method of choice. To reach this resolution, the SR X-ray beam must be focused, and the technology for doing this is available only for soft X-rays (in the 100-eV range). Soft X-ray microscopy has a number of

Mapping of protein and DNA in bull sperm, using the Stony Brook scanning transmission X-ray microscope (STXM) at the National Synchrotron Light Source. The upper set of images is for a sperm with tail missing, but at higher magnification (scale bar equals two microns). Images were collected at six wavelengths near the carbon K absorption edge, where protein and DNA spectra differ. Images on the left are at one of these six wavelengths. Analysis of all six leads to the protein and DNA maps shown in center and right. (Work of Xiaodong Zhang. Specimen courtesy of Dr. Rod Balhorn, Livermore.)

advantages over other recently developed microscopy techniques (such as scanning tunneling microscopy, atomic force microscopy, scanning electron microscopy), the most important one being the ability to image through thick samples (the other techniques "see" only surfaces of objects). This advantage is most important for biological applications such as imaging live cells in a wet environment.

Another advantage of SR-based soft X-ray microscopy is the ability to tune the energy of the radiation to provide contrast dependent on the chemical makeup of different regions of the sample (chemical contrast). For example, the different chemical makeup of nucleic acids (DNA and RNA) compared to proteins allows for microscopic imaging of the ultrastructure and composition of chromosomes. Even regions of the sample that have similar elemental composition but different chemical characteristics (that is, the atoms occur in different molecules with different bonding patterns) can be distinguished using the microscope as a "microprobe." In this usage, the X-ray beam is focused on a particular point of the sample, and the X-ray absorption spectrum is scanned to identify the chemical makeup at that point. This can be done at a number of points in the sample that appear with different contrast in the microscopic image, characterizing the spatial distribution of materials in the sample.

To move from structure at a biological or anatomical level to structure at a biochemical level, we have to change our focus from imaging to spectroscopy. Now we can take advantage of the short wavelength of X-ray photons to yield molecular structure.

X-RAY SPECTROSCOPY

On a biochemical level, scientists are interested in the structures of biomolecules (proteins, nucleic acids, lipids) and the ultrastructure of various assemblies of these molecules, such as chromosomes, ribosomes, membranes, etc. The availability of a tunable source of X-rays like SR has made a large impact on these studies as well. Just as with the imaging applications already discussed, this tunability allows development of contrast to focus attention on the macromolecule of interest or a portion of it and allow one to distinguish it from its environment. Also, as we narrow down our attention to structure at nanometer or Å (10^{-9}–10^{-10} m) resolution, it is the characteristic sensitivity of X-rays with wavelengths that match this length scale to molecular structure that dominates the information attained.

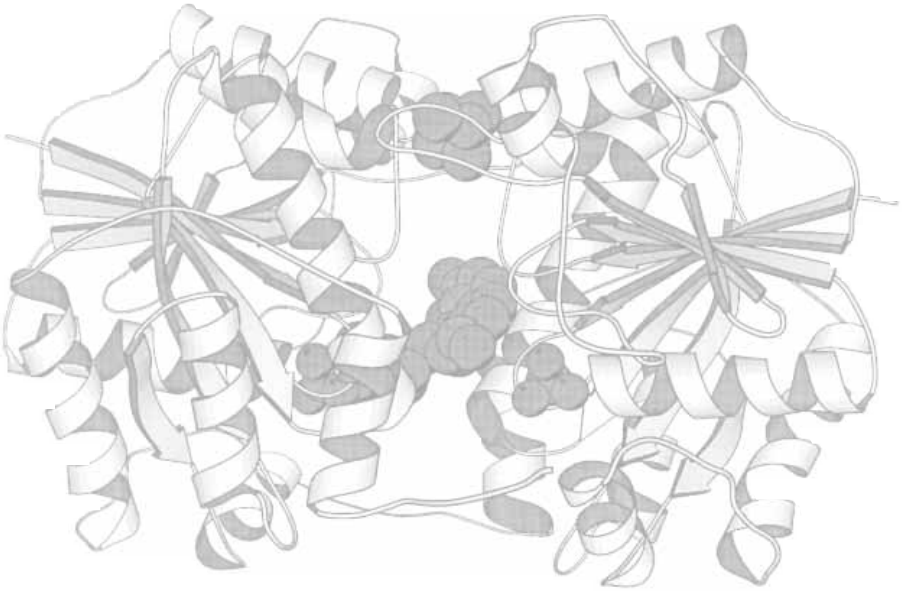

The structure of the Fe protein from the enzyme nitrogenase, solved by X-ray diffraction. The two subunits are joined at the top by the [4Fe-4S] cluster, and the MgATP is expected to bind between the subunits near the bottom. The larger radius of gyration observed for the Fe protein in the absence of MgATP (see text) could arise from separation of the subunits at the bottom. (Figure provided by D. C. Rees, California Institute of Technology.)

X-ray Scattering

One method of obtaining information about biomolecules at molecular resolution is X-ray scattering. In these experiments, X-rays incident upon a sample are scattered from nanometer-sized structures (particles, molecules) in a way that is sensitive to the size and shape of these structures. Placement of an X-ray detector directly behind the sample would measure the transmission of X-rays directly through the sample, but moving the detector away from this position by small angles allows detection of the angle-dependent intensity of scattered X-rays; it is this angle dependence that contains the structural information, leading to techniques referred to as small-angle X-ray scattering (SAXS) and wide-angle X-ray scattering (WAXS). Sensitivity to larger structures increases as the angle decreases, and SAXS has had the largest impact on structure determination of biomolecules (typical protein molecules have length dimensions in the 20–200 Å range).

A globular protein molecule tumbling in solution can be represented as a spherically symmetric structure the size of which can be defined by one parameter, the radius of gyration *(R_g)*. SAXS can be used to measure R_g values for proteins in solution, and several applications of the technique have used this ability to look at changes in the conformation of proteins after some treatment. A recent example of this type of experiment was carried out at SSRL on the iron protein of the enzyme nitrogenase. This enzyme is responsible for nitrogen fixation (reduction of N_2 in the atmosphere to NH_3 that can be assimilated by plants), which occurs in soil bacteria and the root nodules of leguminous plants. The obvious importance of this process to agriculture makes the understanding of nitrogenase function a worthwhile pursuit. Two proteins are involved in the nitrogenase enzyme complex: the "iron (Fe) protein" that contains a cluster of four iron atoms and the "molybdenum-iron (MoFe) protein" that catalyzes the actual reduction of N_2 through the action of an iron- and molybdenum-containing cofactor (FeMoco). The function of nitrogenase requires reducing equivalents (electrons) to be donated from the Fe protein to the MoFe protein, and this electron transfer requires the binding of another cofactor (the magnesium salt of adenosine triphosphate MgATP) to the Fe protein. How the binding of MgATP to the Fe protein affects its interaction with the MoFe protein was the subject of a SAXS study in which a mutated form of the Fe protein that is unable to perform this electron transfer was compared to the natural (wild-type) form. It was found that the wild-type Fe protein had a R_g of 27.2±0.4 Å in the absence of MgATP, whereas addition of MgATP reduced

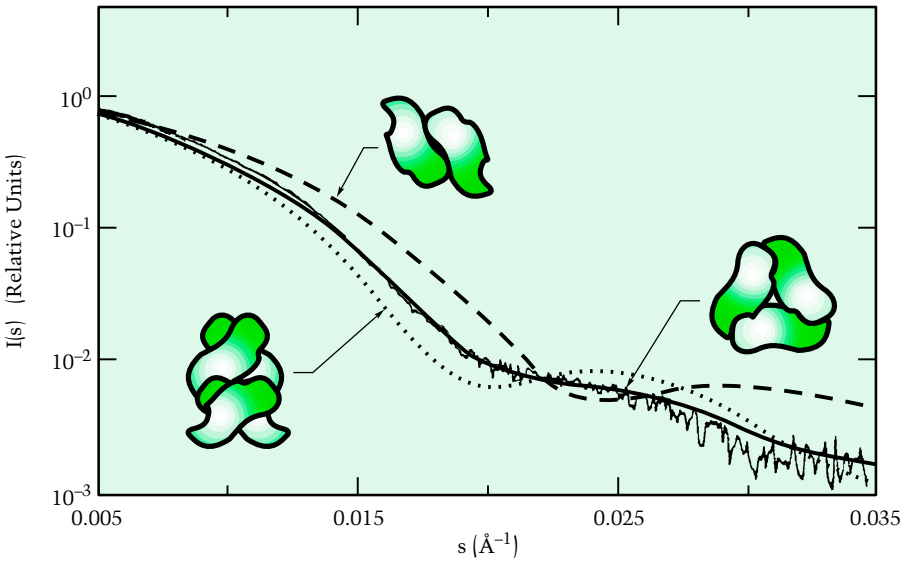

Solution small-angle X-ray scattering profile for the enzyme nitrite reductase from Achromobacter xylosoxidans. The dashed and solid lines represent the simulated data for a set of possible aggregation states (dimer, trimer, tetramer) of this enzyme. These data indicate predominantly the presence of trimers in solution. [J. G. Grossmann et al., Biochemistry 32, 7360-7366 (1993)]

this to 24.6±0.4 Å. By contrast, the mutated form of Fe protein had a R_g of 27.2±0.4 Å, regardless of the presence of MgATP. It appears therefore that a necessary prerequisite for Fe protein interaction with MoFe protein is a MgATP-induced compression of the Fe protein structure. The atomic-resolution structure of the Fe protein suggests that a plausible structural change is the "folding" of the two lobes (subunits) of the molecule around the suspected MgATP binding site.

This experiment points to the potential contribution of SAXS to the study of protein folding in general. One of the major pursuits of protein biochemists is the search for an understanding of how the sequence of amino acid residues in a protein dictates the folding of that protein into a homogeneous globular structure. Such an understanding would revolutionize protein engineering, i.e., the ability to design genetically protein-based enzymes to carry out biotechnologically important reactions. Experiments that can give information about the structure of the unfolded state or intermediate partially folded states of proteins and the kinetics of folding will enhance this understanding. Time-dependent SAXS is a technique that is just beginning to be used for this purpose. In this technique, a stopped-flow apparatus is used to mix rapidly a solution of a protein under conditions favoring the unfolded state with another solution designed to trigger protein folding; SAXS data are collected as a function of time following mixing. Application of this technique to myoglobin (the 0_2-storage heme protein present in vertebrate muscle tissue) showed a rapid conversion (with a half-life of ≈ 1 second) from an unfolded state with R = 32±3 Å to a final state with R_g = 20±2 Å, which is very close to the native state (R_g = 18±1 Å).

Often the functionally viable form of an enzyme is a collection of more than one copy of the protein molecule. These clusters sometimes contain two (a dimer), three (a trimer), or four (a tetramer) protein molecules and are referred to generically as the aggregation state of the enzyme. Newer methods for analysis of SAXS data based on construction of three-dimensional models for the macromolecules followed by simulation of the expected SAXS pattern can lead to determination of the shape and aggregation state of biological macromolecules. One example involves the use of SAXS to determine the solution aggregation state of a copper-containing enzyme nitrite reductase, which is important in denitrification. Early molecular weight determinations suggested a dimeric enzyme in solution, but the crystallographic analysis (see figure) of the structure detected a trimer. With the shape of the protein molecule from the crystal structure, computational models of dimers, trimers, and tetramers were tested by simulating the expected SAXS profiles and comparing them with the observed SAXS data.

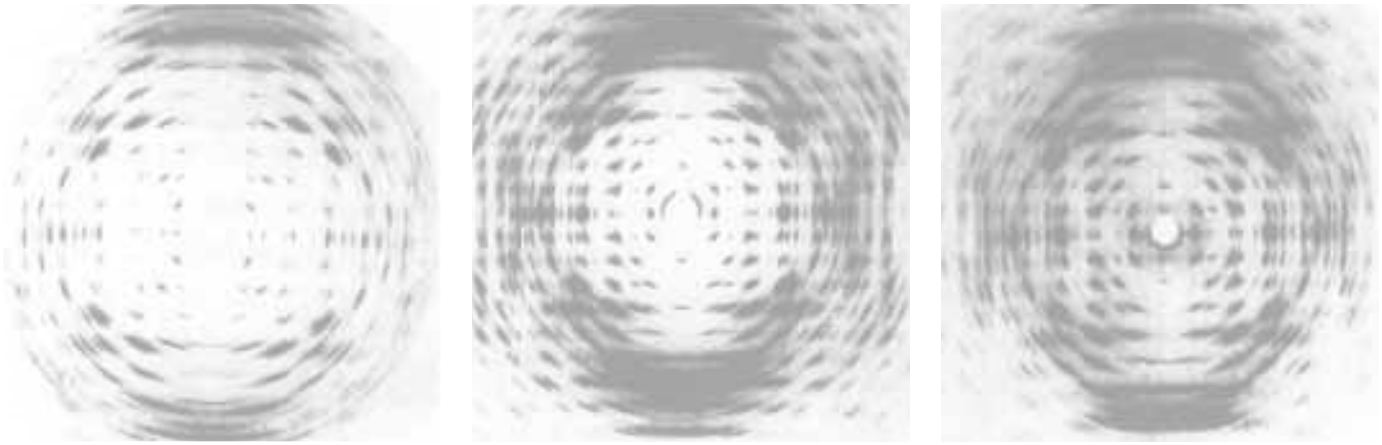

It was clearly demonstrated that only a trimeric arrangement of protein molecules could accurately simulate the observed SAXS data, convincing proof for the existence of trimers in solution as well as in crystals.

Membrane X-ray Diffraction

Another area of biochemical research that is impacted by X-ray scattering experiments is the study of phase transitions in lipid membrane bilayers. The goal behind these studies is to elucidate the nature of localized structural changes that must occur in biological membranes to allow various transmembrane transport functions to occur. Scientists are studying model bilayer systems that have more easily interpretable simple phase transitions by using SR X-rays. In these studies, regular two-dimensional membranes are constructed from component lipid molecules, resulting in well-defined "diffraction" peaks as opposed to the smoothly varying angle-dependent scattered intensity observed in SAXS. Different lipid arrangements (phases) give rise to different sets of diffraction peaks which can be followed as a function of temperature or time following a temperature jump.

Fiber X-ray Diffraction

One-dimensional long-range orientation of biomolecules (into fibers) can also give rise to X-ray diffraction, and this is the basis for a large number of experiments designed to understand the molecular details of muscle contraction and the structure of fibrous proteins (e.g., the connective tissue collagen) and nucleic acids (polynucleotides). Muscle contraction involves the sliding of actin molecules in thin filaments past the thick filaments that are composed of molecules of myosin. The structures of the relaxed, tensioned, and contracted states of muscle fiber bundles or even single fibers can be investigated by X-ray fiber diffraction techniques. Control of this contraction by Ca^{2+} and ATP has also been investigated, the latter in a time-resolved experiment in which ATP generated instantaneously by a light-induced chemical reaction induces contraction which is then followed with sub-millisecond time resolution. Fiber diffraction has also been employed in structural investigations of double-helical DNA molecules. In particular, transformation of a DNA fiber from one conformation (D form) to another (B form) can be induced by humidity changes and has been followed by monitoring characteristic changes in the fiber diffraction pattern. In another experiment, the location of cations (Rb^+, K^+, Li^+) in the double helix was deduced by interpreting changes in the fiber diffraction pattern. The interpretation took advantage of the much better X-ray scattering from Rb^+ compared to Li^+. A better understanding of

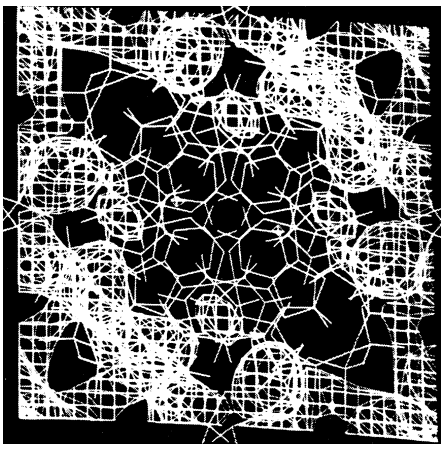

Fiber diffraction patterns obtained at the SRS in Daresbury on fibers of the D form of DNA The alkali metal cation neutralizing the DNA phosphate backbone has been isomorphously replaced with rubidium (top left), potassium (top center), and lithium (top right), altering the diffraction pattern. Comparison of the rubidium to the lithium diffraction patterns allows a calculation of a Fourier difference map that locates the positions of the alkali metal cations (lower frame; the "wire-mesh blobs" indicate extra electron density in the rubidium compared to the lithium structure). [From W. Fuller, V. T. Forsyth, and A. Mahendrasingam in Synchrotron Radiation and Biophysics *(S. S. Hasnain, Ed.), Ellis Horwood: Chichester, 1990, pp. 201-222.]*

Crystallographically determined structure of the enzyme trypanothione reductase, which is the target for drug design in the control of sleeping sickness trypanosome parasites (see text). The two areas of dark spheres on the left (and behind the right) of the molecule are the substrate analogs that occupy the active site of this enzyme. [See Eur. J. Biochem. 213, *67–75 (1993). Figure generated with MolScript, P. Kraulis,* J. Appl. Crystallogr., 24, *946–950 (1991)]*

DNA conformations and interaction with physiological cations (K^+, Mg^{2+}, Ca^{2+}) should eventually allow the definition of DNA conformational changes that influence regulation of transcription and translation (the synthesis of proteins from genetic material).

Single-Crystal X-ray Diffraction

These X-ray scattering and fiber diffraction techniques give information about the overall size and shape of biological macromolecules, but when it is feasible to grow single crystals of these macromolecules, X-ray diffraction can be used to obtain a near-atomic resolution (in the few Å range) structure (a crystal structure) that provides much more information. Knowledge of the structure of an enzyme at this level allows researchers to identify the chemical characteristics of the protein residues in the "active site" of the enzyme and helps them predict how chemical transformations are catalyzed by the enzyme. It may also allow the design of specific potent inhibitors of the enzyme's activity; for example, inhibition of enzymes that are crucial for the growth or infectiousness of pathogens (viruses, bacteria) might arrest the development of the disease that they cause. This rational (structure-based) drug design is a major component of the research efforts of many pharmaceutical companies. A crystal structure may also be the first step in a process known as structure-based protein engineering. Geneticists' ability to alter the gene that codes for a particular enzyme allows for engineering enzymes to be stable at higher temperatures or to carry out new chemical reactions, both of intense biotechnological interest. Knowing the structure of an enzyme allows the researchers to focus on the important residues to alter in these engineering attempts.

Single crystals consist of a repeating three-dimensional lattice of molecules, and this long-range order allows the diffraction of X-rays at discrete angles, generating a diffraction pattern that can be Fourier transformed into a map of the electron density of the molecules in the crystal. The atoms and bonds of the molecule then must be fitted into this electron density map in a process known as refinement. With considerable effort, which traditionally involves binding heavy metals to the macromolecule to act as landmarks in the electron density map, this process yields the atomic-level structure (the position of each atom) of the macromolecule. Although this process can be accomplished with laboratory X-ray sources, SR has made an impact in a number of ways. First, the intensity of the SR-based X-ray source allows data to be collected much more quickly, before the single crystals have time to degrade because of X-ray induced damage. The intensity and collimation of the SR X-rays also allow diffraction data to be collected and crystal structures to be solved for smaller crystals than required for laboratory-based X-ray sources. Most importantly, the ability to change the wavelength (the tunability) of the SR X-ray beam has had a major impact on macromolecular X-ray crystallography. It has allowed the development of a technique known as MAD (multiple-wavelength anomalous dispersion) that uses diffraction data collected at wavelengths near the X-ray absorption edge of one or more heavy atoms in the macromolecule to facilitate the experimenter's ability to "phase" the diffraction data (part of the transformation to the electron density map) without having to bind exogenous heavy atoms. A general approach has been recently developed by Wayne A. Hendrickson and coworkers at Columbia University for recombinant proteins (proteins which are made by incorporating their cloned genes into another host for production) in which methionine amino acid residues (which contain a sulfur atom in their natural form)

are replaced by selenomethionines (which contain a selenium atom in place of the sulfur), and X-rays just below and above the Se K X-ray absorption edge are used in the MAD technique.

As an example of a project involving rational drug design, SR was used to solve the crystal structure of the enzyme trypanothione reductase, an enzyme that is critical for the metabolism of the trypanosome, a protozoan parasite that causes sleeping sickness. Since humans and domestic animals that are infected by this parasite do not have this enzyme, it is a good target for the selective action of a designed drug. The first step in this project was to solve the crystal structure of the enzyme (requiring SR owing to the small size of the crystals obtainable) in the presence of one of the natural substrates. The substrate serves as an accurate indicator of the active site of the enzyme, which will then be the target for designing inhibitors that will bind tightly to the active site and block substrate access. Without the products of this enzymatic reaction, the trypanosome will die, and the designed inhibitor may become the next-generation drug for treating trypanosomal infection.

Laue X-ray Diffraction

Although the static structures resulting from standard X-ray diffraction studies hold significant information about enzyme active sites, these structures cannot yield the most important information regarding the dynamics of the enzymatic reaction itself. The future holds considerable promise about the ability to perform "kinetic crystallography" in which diffraction patterns are collected within milliseconds as snapshots of the entire enzyme structure during the course of the enzymatic reaction. Referred to as Laue diffraction, the most promising technique involves the use of polychromatic rather than monochromatic SR, so that a large number of lattice planes in the sample give rise to diffraction spots, generating a relatively complete set of diffraction data in a single shot. With fast photochemical methods of releasing caged substrates or cofactors contained within the crystal in milliseconds, the Laue method could allow scientists to track the course of an enzymatic reaction using structures at atomic resolution.

X-ray Absorption Spectroscopy

Although over 100 new macromolecular crystal structures are appearing each year, not every enzyme is amenable to this level of structural characterization; the most common difficulty is the inability to grow suitable crystals of your favorite enzyme. For metalloenzymes, one need not despair since the availability of SR has also driven the revival of the technique of X-ray absorption spectroscopy (XAS) that can give some structural information about metal sites in enzymes for non-crystalline samples (e.g., in frozen solution). In most metalloenzymes, this is very useful since the metal is usually part of the active site, the "business end" of the macromolecule. The structural information from this technique comes from analysis of the EXAFS (extended X-ray absorption fine

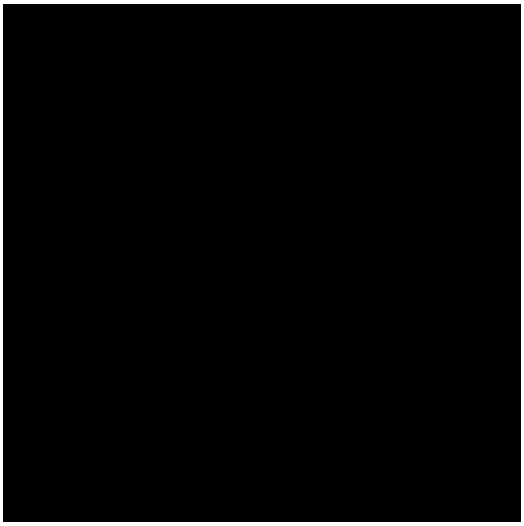

White radiation Laue diffraction pattern from a single crystal of the protein isocitrate dehydrogenase (IDH) from E. coli (IDH is an enzyme that catalyzes the conversion of isocitrate to α-ketoglutarate and CO_2) recorded on SSRL beam line 10-2. The X-ray brightness of BL 10-2 is sufficient for diffraction patterns of this type, containing many thousands of usable diffraction peaks, to be recorded in a few tens of milliseconds on photographic X-ray film, and in only a few milliseconds on imaging plates. (Imaging plates are becoming the detection method of choice for SR X-ray diffraction owing to their large format, high resolution, high dynamic range, sensitivity, and reusability.) This provides the possibility of time-resolved studies in protein crystallography. The photograph was taken by Barry L. Stoddard of the Fred Hutchinson Cancer Research Center, Seattle, and R. Paul Phizackerley and S. Michael Soltis of SSRL/SLAC.

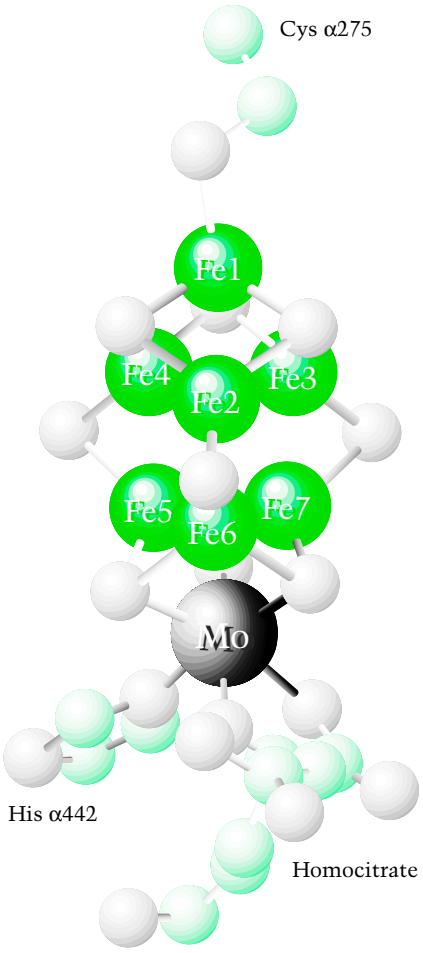

The structure of the iron-molybdenum cofactor (FeMoco) of the enzyme nitrogenase solved by X-ray diffraction. This is the cluster at which N_2 reduction is believed to take place. X-ray absorption spectroscopy successfully defined the Mo-Fe, Mo-S, Mo-O, Fe-S, and Fe-Fe distances before the structure was solved by X-ray diffraction, but was unable to predict the exact arrangement of the atoms in three-dimensional space. (Figure provided by D. C. Rees, California Institute of Technology.)

structure) which consists of energy-dependent oscillations in the absorption by the metal of X-rays with energies just above the metal's K absorption edge. In essence, the photoelectron produced by metal absorption of an X-ray photon scatters from nearby electron density, probing the presence of other atoms in the vicinity of the metal. What results is a "radial map" of the metal environment with information about distances and types of atoms in the neighborhood. This technique can define the protein residues that bind the metal atom, define the number of residues bound, and detect the binding of substrates or inhibitors to the metal. This sort of information is very useful in the absence of a three-dimensional structure of all atomic positions in helping define the active site of the metalloenzyme.

As an example, consider the nitrogenase enzyme mentioned earlier. The MoFe protein of this enzyme complex contains a FeMo cofactor where the substrate N_2 reacts. The structure of this metal cluster was probed by EXAFS years before the crystal structure became available. Although the EXAFS data did not give a complete picture of the structure of this cluster, all the essential metrical details from the Mo EXAFS analysis were correct. The recent solution of the crystal structure of the MoFe protein has opened up the possibility of understanding the chemical mechanism of nitrogen fixation, the first step toward engineering this ability into crops that could then produce their own fertilizer.

SR can also be used to probe the electronic structure of metals in biological molecules. In XAS, close examination of the K X-ray absorption edge region can reveal peaks and shoulders just before the edge arising from electronic excitation from the 1*s* orbital to valence orbitals. Analysis of this region of the spectrum (sometimes referred to as XANES, X-ray absorption near-edge structure) can yield information about the electronic structure and symmetry of the metal site. Certain symmetries are correlated with metal-site reactivity and so can aid in structural and functional characterization of the metalloenzyme.

As for many of the other SR-based techniques discussed, time-resolved XAS holds promise for being able to watch metalloenzyme active sites in action. Photochemical release of substrate or photolysis of metal-bound inhibitor might be used as a trigger to initiate reactions that can then be followed by collection of XAS data on a sub-millisecond timescale. The SR intensity and detector capability required for such experiments will become available during the development of the next-generation SR sources.

As one can see from this summary, synchrotron radiation has had a tremendous impact on the field of structural biology. In addition to being able to collect X-ray based data more efficiently using existing techniques, new techniques have been developed that were not possible without SR. As we move into the next millenium, look for another revolution in the development of temporal resolution that will allow SR-based techniques to examine not only the *structure* but also the *function* of biological systems.

LOOKING DEEPER INTO THE PROTON

by FRANZ EISELE
and GÜNTER WOLF

Electron-proton collisions at higher energy show a rapid increase of soft quarks and gluons in the proton.

For more than forty years high energy electron beams have been used as an ideal probe for measuring the internal structure of extended objects like nuclei and their building blocks, the proton and the neutron. At energies of several GeV one begins to resolve substructures in the proton.The highlight of these electron-scattering experiments was the discovery at SLAC in 1969 that the proton is actually made of pointlike constituents which later were identified as quarks and gluons.

The electron-proton collider HERA, which has been operating since the summer of 1992 at the German research center DESY in Hamburg, boosts the resolution power of electron-scattering experiments by more than an order of magnitude and allows a much deeper look inside the proton. It may even provide the possibility of seeing the structure of quarks and electrons if they themselves are not truly pointlike.

The basic concept for unraveling the structure of matter by scattering experiments is straightforward. A beam of energetic and point-like particles (= test particles) is directed against a target material, and the energies and angular distributions of the scattered beam particles are measured. An early example is the experiment of Rutherford and his coworkers Geiger and Marsden (1909–1913), who scattered alpha particles (helium nuclei) from metal foils. The observed angular distribution of the alphas led to the conclusion that atoms are almost all empty space but possess a small and massive core against which the alphas are occasionally scattered at large angles.

The object size Δ that can be resolved in the scattering process is determined by the kick or momentum Q that the test particle transfers to the target particle, $\Delta = 0.2/Q$, where Q is measured in GeV and Δ in fm (1 fm = 1 fermi or 1 femtometer = 10^{-13} cm). The maximum momentum transfer Q (and hence the resolution) increases with the energy of the test particle. In the Rutherford experiment the incident alpha particles were provided by radioactive decay and had kinetic energies in the MeV range, thus permitting the identification of objects as small as a few fm. The core or nucleus of the atom was found to have a radius smaller than 30 fm, or about 10,000 times smaller than the whole atom.

The structure of the individual nucleons (protons and neutrons) that make up the nucleus can best be explored with beams of leptons, such as electrons, muons and neutrinos which are produced at high energy accelerators. These particles are themselves pointlike—as far as we know—and this is one of the reasons why their interactions with other particles are well understood. Experiments performed in the late 1950s with elastic scattering of electrons around 1 GeV, for instance at Stanford, showed that nucleons are not pointlike but are instead extended objects with a radius of about 0.8 fm. Particle physics was revolutionized in the late 1960s when the SLAC-MIT group discovered Bjorken scaling which showed that nucleons are made of even smaller, apparently pointlike constituents, called partons. The evidence came from 20 GeV electrons striking a nucleon target and scattering inelastically at large angles. This was reminiscent of Rutherford's observation but now seen at the much smaller resolution scale of a tenth of the proton radius. The pointlike parton constituents were later found to match the properties of the quarks that had previously been postulated by Gell-Mann and Zweig.

The results from the SLAC-MIT experiment were explained by the quark-parton model of Feynman and, together with further lepton scattering experiments, led to the formulation of Quantum Chromodynamics (QCD), the theory that describes the strong interactions in terms of a new force acting on color charges in much the same way as the electrodynamic force acts on electric charges. Nucleons are made of quarks and gluons which carry color charge. Quarks possess, in addition, electromagnetic and weak charges. Gluons are responsible for binding quarks together in the nucleon in a way that is similar to photons binding electrons and the nucleus together to form an atom. The observable strongly interacting particles are color neutral; similarly, atoms are electrically neutral. Several generations of lepton-scattering experiments have since measured the momentum distributions of quarks and gluons inside the proton and neutron, and they have made invaluable contributions to our understanding of the basic weak, electromagnetic and strong interactions.

As an example, in contrast to the electromagnetic interactions, the weak interactions that are responsible for the radioactivity from nuclear beta decay are mediated by the exchange of any of three massive, charged or neutral vector bosons $W^{\pm}$ and Z^0, with 85 and 100 times the mass of a proton respectively. Their study as well as the search for new currents and the question of whether quarks and leptons are composite particles called for much higher Q^2 values. Prior to HERA, the lepton beam in these experiments was directed onto a stationary (fixed) target containing neutrons and/or protons. A maximum energy of 600 GeV was reached at Fermilab for muon and neutrino beams, thus providing lepton-nucleon center of mass energies of 30 GeV and momentum transfers of 20 GeV, which is equivalent to a resolution of $\Delta = 10^{-2}$ fm. To gain an order of magnitude in resolution with the same technique would require increasing the lepton energy by two orders of magnitude to 50,000 GeV, for example by lining up a thousand SLAC-type linear accelerators, each 3 km long, one behind the other. This does not seem to be a practical solution.

THE HERA MACHINE

At HERA the equivalent electron beam energy of 50,000 GeV is achieved by colliding 30 GeV electrons head-on with 820 GeV protons, which results in a center of mass energy of 300 GeV. (E_e, E_p are the energies of the electron and proton beams.) The two beams are accelerated and stored in two independent rings of 6.3 km circumference mounted on top of each other. Magnetic guide fields keep the beams on orbit. For the electron beam, standard room-temperature electromagnets are adequate. For the proton beam, superconducting magnets had to be built which operate at a temperature of 4.3 K and provide a field of 4.7 Tesla.

The rate of collisions between electrons and protons is given by the product of the cross section σ for electron-proton scattering and the luminosity L of the collider, $n = \sigma \times L$. The luminosity depends on the particle densities in the two beams. In fixed-target experiments proton densities as high as 10^{23} per cm^2 can readily be achieved. Not so in a collider: the proton density in HERA is nine orders of magnitude smaller. In order to compensate, at least partially, for the lower density, protons and electrons are stored in up to 210 bunches each, which counter-rotate at nearly the velocity of light in the two rings and cross each other every 96 nanoseconds at two points. The design luminosity of $L = 1.5 \times 10^{31}$ cm^{-2}s^{-1} leads to 15 events per second for a cross section of 10^{-30}cm^2 (=1μb). The peak luminosity has risen steadily since the start of experimentation in June 1992 to 5×10^{30} cm^{-2}s^{-1} in late 1994. The integrated luminosity delivered per experiment (see figure) illustrates the progress made in understanding the machine. In 1994 the total luminosity reached 6 pb^{-1} (= 6×10^{36} cm^{-2}s^{-1}) which yields 6 million events for a cross section of 1 μb. These data are now under analysis. By 1996 an annual luminosity of 30–50 pb^{-1} is expected. The physics results that will be discussed below have been

Inelastic Electron-Proton Scattering

In a simple picture of inelastic electron-proton scattering the electron emits a virtual photon (γ^*) which transfers a kick Q and an energy ν to the proton in the proton rest system (see figure below).

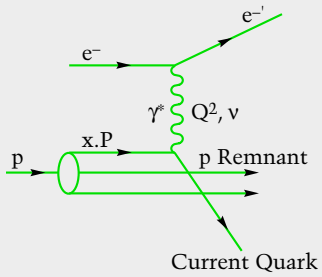

The exchanged photon, which can be thought of as a neutral current flowing from the electron to the proton, is virtual and has a mass squared ,

$$m_\gamma^2 = -Q^2.$$

If Q is large, so that Δ is small compared to the radius of the proton,

$$Q >> 1 \text{ GeV},$$

the photon does not interact with the proton as a whole but rather with one of its quarks. (Since the photon couples only to electromagnetic charges, it does not interact directly with gluons, which are electrically neutral.) In the simplest case, the basic process is the elastic scattering of an electron on a quark. The quark carries a fraction x of the proton momentum which is related to Q^2 and ν by

$$x = Q^2/(2\, m_p \nu),$$

where m_p is the proton mass. The struck quark knocked out from the proton as well as the proton remnant left behind carry color charge and cannot directly be observed. Both fragment into jets of strongly interacting particles (hadrons) such as nucleons, pions and kaons. One assumes that at the end of the fragmentation process the color charges from the struck quark and from the proton remnant neutralize each other.

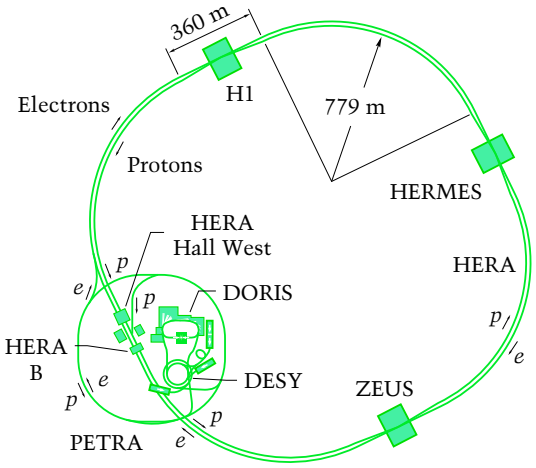

Layout of the HERA collider together with the preaccelerators DESY and PETRA, showing also the location of the experiments.

Development of the integrated luminosity versus time for the data taking in 1992-1994.

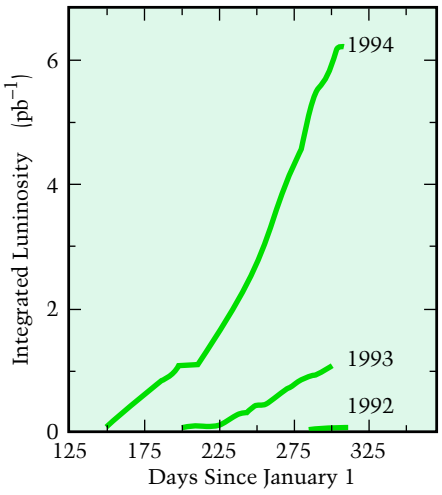

obtained from analysis of the 1993 data, which correspond to a total luminosity of 0.6 pb^{-1}.

An ambitious goal at HERA was the provision of polarized beams of electrons and positrons with spins parallel and antiparallel to the direction of flight. This has been achieved for the first time in a storage ring with polarizations of 60 percent for the electron beam.

EXPERIMENTS AT HERA

Two of the four interaction points are occupied by the general-purpose detectors H1 and ZEUS, which have been taking data since the start of HERA in 1992. At the third point the HERMES detector is under construction for studying the scattering of polarized electrons on polarized protons and light nuclei from a gas jet. The fourth interaction region is earmarked for HERA-B, which will use the halo of the proton beam from HERA to produce B-mesons and to search for CP violation in the B system.

The H1 and ZEUS detectors are designed for optimum precision in measuring inelastic electron-proton scattering. A typical neutral-current event produced via the exchange of a photon or Z exchange is displayed in the figure (facing page). One observes an energetic and isolated electron whose transverse momentum relative to the beam axis is balanced by a set of strongly interacting particles, called hadrons, most likely stemming from the struck quark. The energy deposited near the proton direction stems presumably from the proton remnant. The two fundamental variables Q^2 and x which characterize the scattering process can be determined from the energy and angle of either the scattered electron or of the hadron system.

In the case of a charged-current event produced by W^+ or W^- exchange, the outgoing lepton is a neutrino, $e^- p \rightarrow \nu X$, which leaves no trace in the detector. Such events must be recognized by the missing transverse momentum carried away by the neutrino. The example shown in the figure on the facing page has a transverse momentum imbalance which indicates that the neutrino escaped as shown with an energy of about 200 GeV. For charged-current events, Q^2 and x can only be determined from the hadron system. The identification of these events requires a detector that covers the full solid angle without gaps and holes, so that particles like photons, K mesons and neutrons cannot escape undetected.

In view of the emphasis on the energy and angle measurements of electrons and hadrons, it is no surprise that the H1 and ZEUS detectors are determined by their choice of calorimeter. A calorimeter measures the energy and direction of particles by total absorption and the localization of the energy deposition. Both experiments use a sampling calorimeter, where layers of absorber and detector alternate. Hadrons, photons and electrons that hit the calorimeter produce showers of secondary particles in the absorber plates. The number of secondaries is counted in the detector layers and is a measure of the energy of the incident particle. ZEUS uses depleted uranium plates as absorber, with scintillator for readout, which provides a

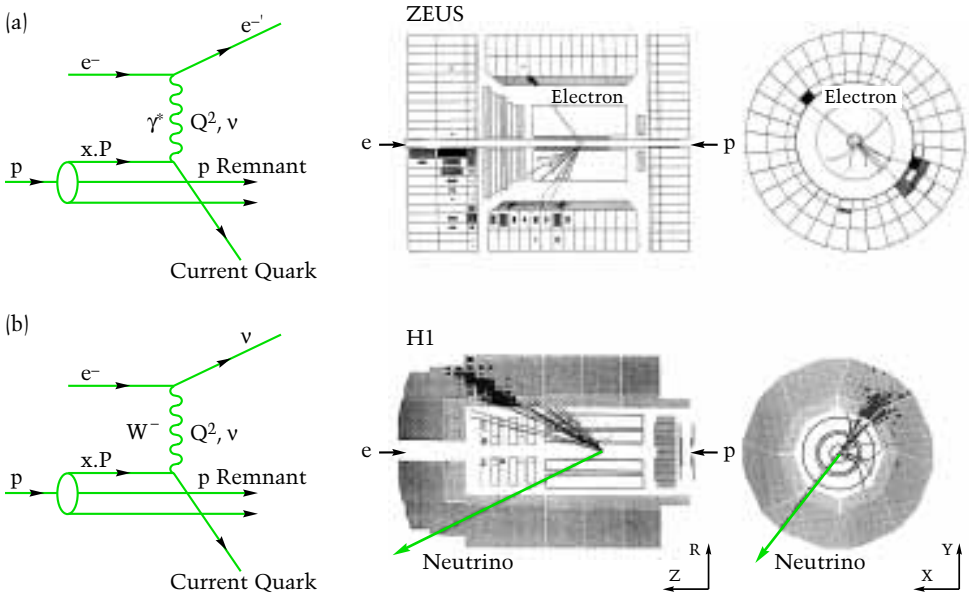

compensating calorimeter with the best possible energy resolution for hadrons. "Compensation" means that electromagnetic particles (electrons, photons) and hadrons of the same energy yield the same signal. The slight radioactivity of the uranium provides a stable calibration. With the exception of the forward and rear beam holes, the calorimeter covers hermetically the full solid angle. H1 chose liquid argon for readout, and lead and steel plates as absorbers. Liquid-argon readout offers a stable and simple calibration and allows a fine transverse and longitudinal segmentation of the readout. The calorimeter is noncompensating, but by analyzing the shower profiles equal signals for electrons and hadrons can be obtained.

In addition to the calorimeter, both detectors are equipped with wire chambers around the collision point for accurate tracking of charged particles. A superconducting solenoid provides a high magnetic field for measuring particle momenta from their observed track curvature. The high resolution calorimeter is surrounded by the iron yoke, which is instrumented with wire chambers for the detection of leaking showers and for the identification of penetrating muons. In addition, the first 100 meters of the collider rings upstream and downstream of the central detector are used as spectrometers. They are instrumented with calorimeter and tracking devices for the detection of protons and neutrons produced in the proton direction, and of photons and electrons produced in the electron direction. The latter serve for measuring the luminosity and for tagging of photoproduction.

The high beam-crossing rate and the large number of electronic channels in both experiments required the development of new concepts for acquisition of the data. The signals from the 200,000 to 300,000 channels, amounting to several Terabytes (10^{12} bytes) of information per second, are stored every 96 nsec in analog or digital pipelines that can hold the results from 25 to 50 beam crossings. In parallel, signals obtained by summing over many channels are stored in trigger pipelines and analyzed in giant parallel processors to select the interesting events, which are finally recorded on tape.

Events from electron-proton scattering observed in the H1 and ZEUS detectors in views parallel (center) and perpendicular (right) to the beam axis. Tracks of charged particles are reconstructed from hits registered in the inner tracking chambers. The energy deposition from particles is measured by the calorimeter; energy desposits in a readout cell are displayed by rectangles. Top row: a neutral current event, ep → eX, as measured in the ZEUS detector with Q^2 = 5300 GeV^2. The transverse energy of the electron is balanced by a hadron jet at large angle from the current quark. In addition, there is a substantial energy deposition near the proton beam direction stemming from the proton remnant. Bottom row: a charged current event, ep → νX, as observed with the H1 detector at Q^2 = 20,000 GeV^2. There is a jet emitted to one side of the detector whose transverse momentum is not balanced by other detected particles, indicating the emission of an undetected neutrino to the opposite side (solid green line).

THE JANUS HEAD OF THE PHOTON

"Die ganzen 50 Jahre bewußter Gruebelei haben mich der Frage was sind Lichtquanten nicht naeher gebracht." "The whole 50 years haven't brought me closer to the question of what is the nature of light quanta," wrote A. Einstein in 1951, in reference to the experimental observation that photons can behave both as waves and as particles. HERA is a copious source of photons with mass-squared values so close to zero that they can be regarded as real photons. The photon energy measured in the

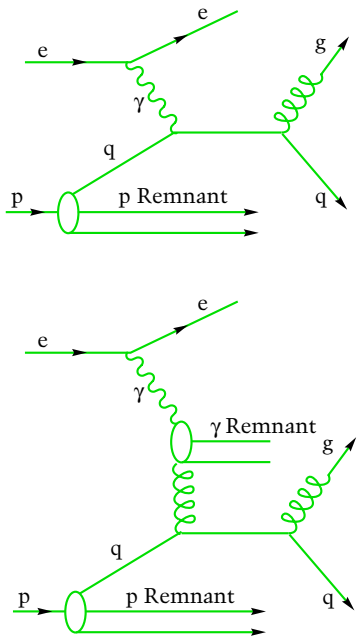

Photoproduction at HERA by the emission of an almost real photon ($Q^2 \cong 0$). Top: A direct photon process where the photon interacts directly with a quark from the proton, producing a quark and a gluon which turn into two jets emitted at large angles. In addition, there is a jet resulting from the proton remnant which has the direction of the incoming proton. The total energy of the photon participates in the hard interaction, $x_\gamma = 1$. Bottom: A resolved photon process where the photon resolves into quarks and gluons. One of the gluons interacts with a quark from the proton, leading to two large angle jets plus the proton remnant jet in the proton direction and the photon remnant jet in the photon direction. Only a fraction of the photon energy participates in the hard scattering, $x_\gamma = 1$.

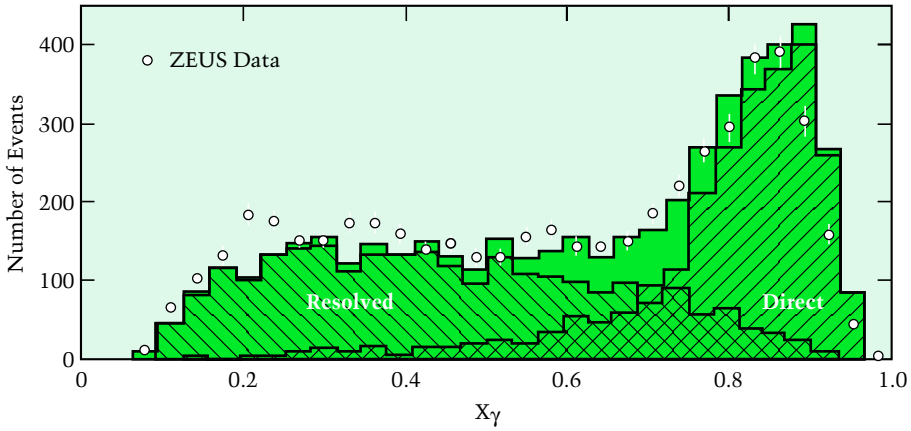

The fractional energy x_γ of the photon participating in hard scattering of photoproduction leading to two large-angle jets. Two distinct components are seen: the direct-photon contribution peaking at large values of x_γ, and the resolved-photon contribution with smaller values of x_γ.

proton's rest system can be as high as 50,000 GeV. The photon interacts with the electrically charged quarks in the proton. This is called a direct photon interaction. However, Heisenberg's uncertainty principle allows the photon for a short time also to fluctuate into a quark-antiquark pair. Although the time is short, it is long enough for a photon with HERA energies to travel a distance which is many hundred proton radii long. The quarks in turn emit gluons so that the photon looks like a cloud of quarks and gluons which then interacts with the quarks and gluons of the proton. This is dubbed a *resolved* photon interaction. The large photon energies available at HERA allow one to distinguish between the two modes of interaction by selecting events from hard scattering with two energetic and large angle jets. From the energies and directions of the two jets one can determine whether the *total* energy of the photon ($x_\gamma = 1$) participated in the collision with a constituent of the proton as for direct interactions; or alternatively whether only a fraction of the energy ($x_\gamma < 1$) participated, as for resolved interactions. The frequency distribution of the energy fraction (see figure) shows clearly the presence of both processes through a direct peak near $x_\gamma = 1$ and a second resolved component at smaller x_γ values. This is the first measurement where the interaction of the direct and the resolved photon with a proton has been demonstrated. The observation of resolved photon processes can now be used to measure the partonic structure of the photon, so that HERA becomes also a microscope which explores the interior of the photon.

For the event sample shown the contributions from the direct and resolved photon are of comparable magnitude. This is so because events from hard scattering were selected. Overall, soft-scattering events are much more abundant, and in such events by far the dominant contribution comes from resolved processes where the photon behaves like a bag of quarks and gluons. It might well be said that Einstein had already forseen the split personality of the photon when he said, *"Jeder Lump meint er weiß, was ein Photon ist, aber er irrt sich."* ("Every idiot thinks he knows what a photon is, but he is mistaken.")

THE INFLATION OF SOFT QUARKS AND GLUONS IN THE PROTON

A topic that was not on the top of the agenda when HERA was first proposed, but which has received increasing attention in the last two

The proton structure function F_2 (x, Q^2) as a function of x for fixed Q^2 as measured by the HERA experiments at small x, and by the fixed-target experiment NMC at large x. A strong rise is seen as x tends to zero. The two curves show the expectations prior to HERA for the case that the gluon density at low Q^2 is constant with x (dashed curves) or rapidly rising as $x \to 0$ (solid curves). Both curves describe the fixed-target data.

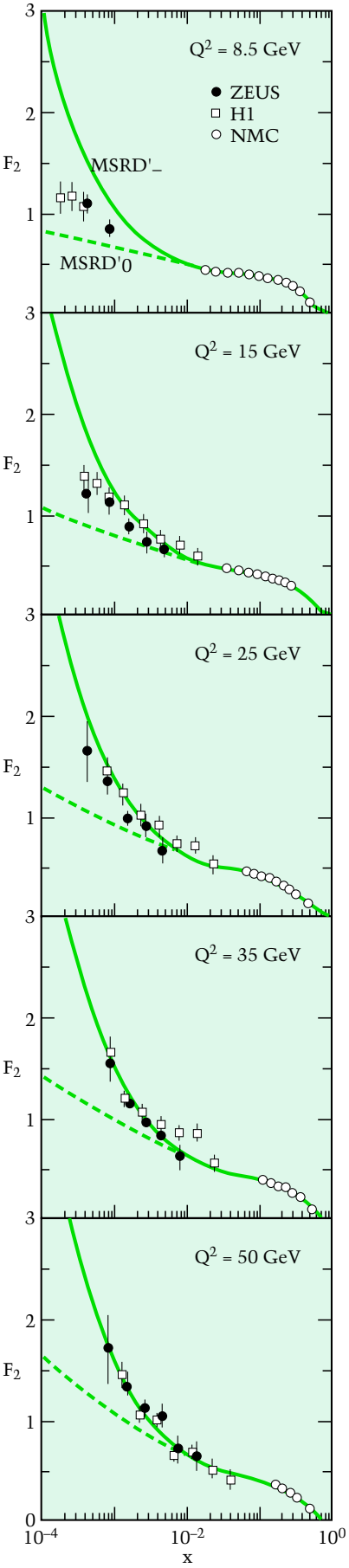

years and has led to the first surprise from HERA, comes from the measurement of very soft partons. The proton contains at least two *up* quarks and one *down* quark, called the valence quarks, and gluons which provide the binding force between them. Gluon annihilation into quark-antiquark pairs and radiation of gluons from quarks both increase the number of partons in the proton, so that on average each of these partons carries only a small fraction x of the total proton momentum. Individual partons become visible if the momentum kick Q they receive is above 2 GeV. The high energies provided by HERA permit observation at this Q value of partons that carry as little as $x = 10^{-4}$ of the total proton momentum, whereas for fixed-target experiments x must be larger than 10^{-2}.

From the measurements made during the 25 years prior to HERA, one had a rather precise knowledge of the parton density for $x > 10^{-2}$, but it was impossible to firmly predict the behavior of the density at much smaller x values. The surprising result from the HERA measurement is best seen in the accompanying figure, which shows the measured x dependence of F_2 for five different values of Q^2. The structure function and hence the density of quarks, which seems to flatten off as x decreases in the range of fixed-target experiments (see the data points from the NMC experiment at $x > 10^{-2}$) suddenly shows a dramatic rise in the HERA region of x below 10^{-2}. An analysis of the change of F_2 with Q has shown that the density of gluons in the proton increases also as x becomes smaller.

The measurement of F_2 can be converted into a measurement of the total cross section for the scattering of virtual photons on protons, $\sigma_{tot}(\gamma^* p)$, which gives a more intuitive picture of what happens. The total center of mass energy W of the photon-proton system for small x is related to x and Q^2 by the relation $W^2 = Q^2/x$. Unlike any known total cross section for real particle scattering at high energies, $\sigma_{tot}(\gamma^* p)$ rises approximately linearly with the total center of mass energy W for fixed Q^2, as shown in the figure on the next page. Another way of saying this is that the virtual photon sees a proton that becomes more

Density of Quarks in the Proton

The density of quarks, $q(x,Q^2)$, in the proton can be obtained from the structure function of the proton,

$$F_2(x,Q^2) = \Sigma_q\, e_q^2\, x \times q(x,Q^2),$$

which is directly measured in deep inelastic electron-proton scattering. Here, e_q is the electric charge of the quark q; for instance, $e_q = (2/3)$ for *up* quarks and $(-1/3)$ for *down* quarks The measured quark distributions depend on the resolution and therefore on Q. As Q is increased, the probing electron resolves more and more of the substructure in the proton, with the main effect being that an increasing number of soft quarks and gluons should be found.

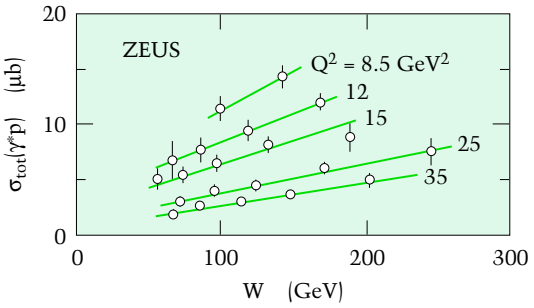

The total cross section for virtual photon-proton scattering, $\sigma_{tot}(\gamma^* p)$, for fixed Q^2, seen to rise approximately linearly with the center of mass energy W.

and more opaque (or "black") as W increases, as a result of the growing number of low-x partons.

This was not entirely unexpected. Some of the QCD predictions for the soft parton region included a strong rise of the parton densities for x approaching zero, using the so-called Lipatov evolution equation. All evolution schemes which have been derived so far for small x invoke different approximations, and their validity is not clear. While the question of which evolution equation may be valid at small x is hotly discussed among experts, there is another interesting and even more fundamental question: *will HERA see the condensation of partons at small x?* The strong increase of the quark and gluon densities observed at HERA provokes the question of whether these parton densities can continue to rise at the same rate forever. The answer is clearly no, since otherwise the total photon-proton cross section would eventually violate unitarity. What will presumably happen is that the parton densities become so high that the partons interact and recombine before they are hit, leading to a saturation of the parton densities. According to Gribov, Levin and Ryskin there is a good chance that the transition from free quarks or a quark "gas" to a quark "liquid" is within the kinematic reach of the experiments at HERA. The probability is even higher when the parton densities do not uniformly populate the proton but rather concentrate in a few hot spots, for instance around the valence quarks.

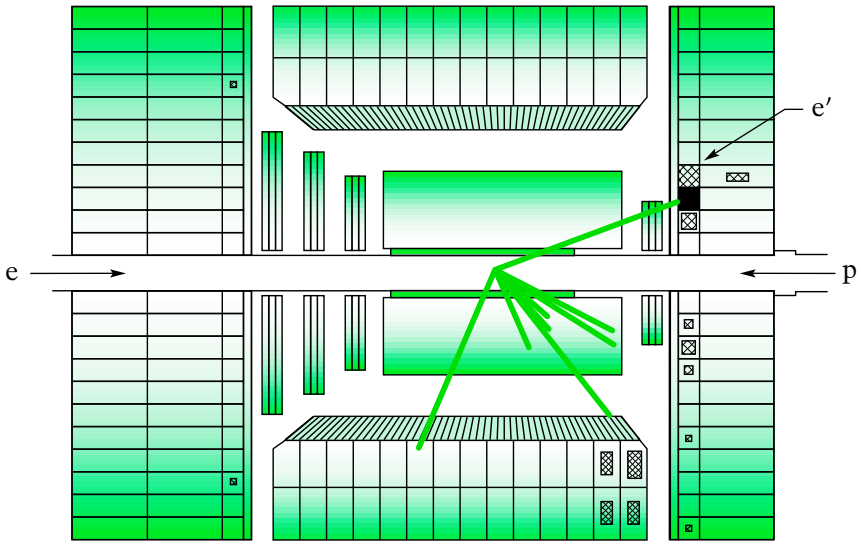

Diffractive event produced by inelastic electron-proton scattering at Q^2 = 58 GeV. The diffractive nature is seen from the absence of energy deposits near the proton direction.

DIFFRACTION OF VIRTUAL PHOTONS

Diffraction is a well known phenomenon in optics. A striking example is the observation that a light beam which is intercepted by a small disc shows maximum intensity directly behind the center of the disc where no direct light rays can go. It has been known for quite some time that a similar diffraction behavior is observed when energetic photons scatter elastically on a proton or produce a vector meson with the same quantum numbers as the photon. These diffractive processes, which are also prominent in hadron-hadron interactions, are phenomenologically described by the exchange of a colorless, neutral object called the Pomeron. So far the nature of the Pomeron is not understood, and a quantitative description of diffractive processes in the framework of QCD is not possible.

The observation of a new class of diffractive events by the HERA experiments may be the key for understanding diffraction scattering. These so-called "large rapidity gap" events are observed to contribute a sizeable fraction of the total cross section also at large Q^2. Their signature is the production of a massive hadronic system without visible energy flow in the direction of the proton remnant. An example of such an event is displayed in the figure on the previous page (bottom left). It is remarkable for the absence of energy deposition in the forward direction. Since these diffractive events show the same Q^2 dependence as the total event rate, one concludes that their production occurs on constituents in the proton whose size is much smaller than the radius of the proton. However, because of the absence of particle production in the forward direction these constituents cannot be quarks or gluons but must be color neutral and therefore a new type of constituent. It is intriguing to identify them with the Pomeron. These unusual events offer the possibility to study at HERA the nature of diffractive processes as a function of resolving power and energy transfer.

WEAK INTERACTIONS BECOME STRONG AT HIGH ENERGIES

While the charged vector bosons were first observed at CERN in 1983, the effect of the W mass in weak interactions has never been directly seen. The two HERA experiments were able to identify some fifty charged-current events in the 1993 data, where instead of an electron a neutrino was emitted. The value of Q for the majority of these events is comparable to the W mass. The observed event rate can indeed only be understood if a particle with a mass near the W mass is exchanged. Moreover, the comparison with events that have a scattered electron in the final state shows directly and for the first time that the weak interaction becomes as strong as the electromagnetic interaction when Q becomes comparable to the mass of the W, whereas it is about 10^{11} times smaller at the low energies involved in nuclear beta decay. This is a fundamental prediction of the electroweak theory.

OUTLOOK

The strong increase of soft parton densities and the search for saturation effects combined with the chance to test QCD in a new regime will remain a hot subject of HERA physics. The HERA experiments had a first look into the physics at high Q^2. This is an area which will come into full bloom when the design luminosity is reached. It will allow one to probe quarks and electrons for substructure, will provide stringent tests of QCD and will show new pieces of the neutral and charged currents—if there are any. Every step in luminosity will increase also the sensitivity to new particles with masses up to 250–300 GeV hardly accessible at other existing accelerators.

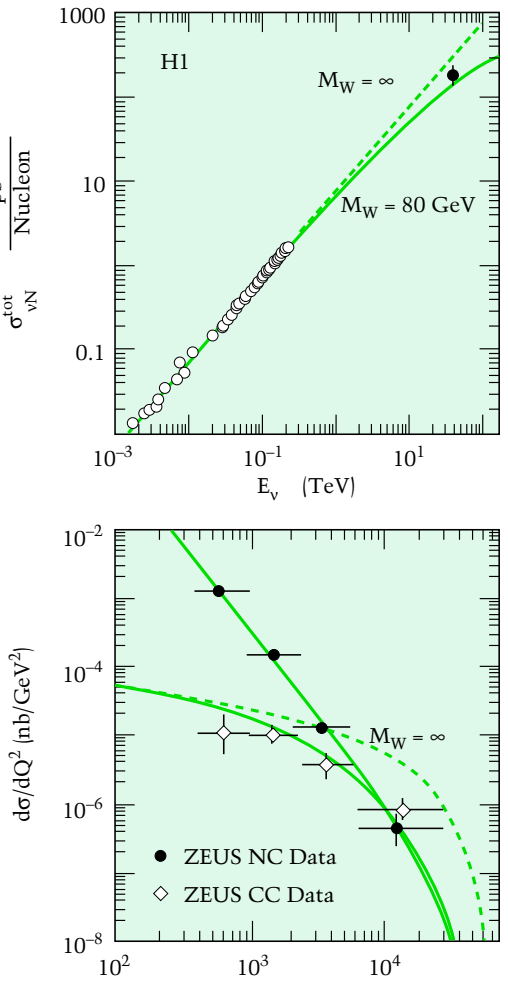

Top: Measurement of the charged-current cross section for ep → νX by H1 translated into the cross section for the inverse process νp → eX at a neutrino energy of 50 TeV and compared to the results from the low energy fixed-target experiments. The straight line (dashed) shows the expectation if the W mass is infinite; the solid line was calculated for a W mass of 80.2 GeV. The finite W mass reduces the cross section at HERA by more than a factor of two, in agreement with the measurement. Bottom: The cross sections for neutral-current (ep → eX) and charged-current scattering (ep → νX) measured by ZEUS become comparable as Q^2 approaches the mass squared of the W (Q^2 = 6400 GeV^2).

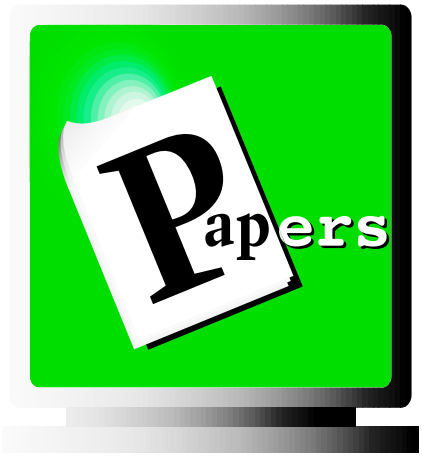

That Shaped Modern High-Energy Physics

by HRVOJE GALIĆ

SPIRES DATABASE SYSTEM at SLAC is a treasure-chest of information. The most popular database is HEP, a joint project of SLAC and DESY libraries. HEP contains almost 300,000 entries with bibliographic data on articles, preprints, and bulletin-board papers in high-energy physics. Since 1974, HEP has tracked the number of times a published high-energy physics article is cited by later works. If you know the exact reference of an article, it is easy to find how many citations the article has in the HEP database.* A citation search may often identify important contributions to a scientific field. The citations in HEP are collected from preprints received by the SLAC library. The library receives between 8,000 and 10,000 preprints yearly, and each of the preprints is a potential source of many citations. Note that HEP *does not* register works cited by journal articles which never appeared as preprints.**

** The database can be accessed and searched on the World Wide Web and via the remote server Qspires. To learn more about the access, write to qspi@slac.stanford.edu*

*** In earlier years, only citations of published journal articles were collected from preprints received by the SLAC library. HEP now also collects citations of bulletin-board papers ('e-prints'). When (and if) a bulletin-board paper is published, citations from the publication phase get added to the citations from the bulletin-board phase.*

HEP Papers with the Most Citations in the HEP (Spires) Database between January 1, 1992 and December 31, 1994

1261 J.J. Hernandez, et al. (Particle Data Group) Review of Particle Properties *Phys. Rev.* **D45**, S1 (1992)

575 J.J. Hernandez, et al. (Particle Data Group) Review of Particle Properties *Phys. Lett.* **B239**, 1 (1990)

465 N. Isgur, M.B. Wise, Weak Decays of Heavy Mesons In Static Quark Approx. *Phys. Lett.* **B232**, 113 (1989)

448 N. Isgur, M.B. Wise, Weak Transition Form Factors Between Heavy Mesons *Phys. Lett.* **B237**, 527 (1990)

422 H.P. Nilles, Supersymmetry, Supergravity And Particle Physics *Phys. Rept.* **110**, 1 (1984)

393 S. Weinberg, A Model of Leptons *Phys. Rev. Lett.* **19**, 1264 (1967)

382 H.E. Haber, G.L. Kane, The Search For Supersymmetry *Phys. Rept.* **117**, 75 (1985)

377 U. Amaldi, W. de Boer, H. Furstenau, Comparison of Grand Unified Theories With ... Coupling Constants Measured at LEP *Phys. Lett.* **B260**, 447 (1991)

373 T. Sjostrand, M. Bengtsson, Lund Monte Carlo For Jet Fragmentation ... Jetset Version 6.3 *Comput. Phys. Commun.* **43**, 367 (1987)

370 P. Langacker, M-X. Luo, Implications of Precision Electroweak Experiments for M(T), ρ^0, Sin^2-θ_w and Grand Unification *Phys. Rev.* **D44**, 817 (1991)

361 E. Witten, On String Theory And Black Holes *Phys. Rev.* **D44**, 314 (1991)

358 M.A. Shifman, A.I. Vainshtein, V.I. Zakharov, QCD And Resonance Physics *Nucl. Phys.* **B147**, 385 (1979)

330 E. Witten, Quantum Field Theory and Jones Polynomial *Commun. Math. Phys.* **121**, 351 (1989)

327 M. Kobayashi, T. Maskawa, CP Violation In Renormalizable Theory of Weak Interaction *Progr. Theor. Phys.* **49**, 652 (1973)

323 Y. Nambu, G. Jona-Lasinio, Dynamical Model Of Elementary Particles *Phys. Rev.* **122**, 345 (1961)

322 M. Jimbo, Q-Difference Analogue of U(G) and Yang-Baxter Equation *Lett. Math. Phys.* **10**, 63 (1985)

317 A.A. Belavin, A.M. Polyakov, A.B. Zamolodchikov, Infinite Conformal Symmetry In 2-D Quantum Field Theory *Nucl. Phys.* **B241**, 333 (1984)

308 J. Gasser, H. Leutwyler, Chiral Perturbation Theory to One Loop *Ann. Phys.* **158**, 142 (1984)

307 H. Georgi, An Effective Field Theory For Heavy Quarks at Low Energies *Phys. Lett.* **B240**, 447 (1990)

301 G. 't Hooft, Computation of Quantum Effects Due to 4-D Pseudoparticle *Phys. Rev.* **D14**, 3432 (1976)

All-Time Favorites—HEP Papers with the Most Citations in the HEP (Spires) Database at SLAC since 1974

4373 S. Weinberg, A Model of Leptons *Phys. Rev. Lett.* **19**, 1264 (1967)
2513 S.L. Glashow, J. Iliopoulos, L. Maiani, Weak Interactions With Lepton-Hadon Symmetry *Phys. Rev.* **D2**, 1285 (1970)
2399 M. Kobayashi, T. Maskawa, CP Violation in Renormalizable Theory of Weak Interaction *Progr. Theor. Phys.* **49**, 652 (1973)
2023 H. Georgi, S.L. Glashow, Unity of All Elementary Particle Forces *Phys. Rev. Lett.* **32**, 438 (1974)
1915 S.L. Glashow, Partial Symmetries Of Weak Interactions *Nucl. Phys.* **22**, 579 (1961)
1894 K. G. Wilson, Confinement of Quarks *Phys. Rev.* **D10**, 2445 (1974)
1610 J. C. Pati, A. Salam, Lepton Number as the Fourth Color *Phys. Rev.* **D10**, 275 (1974)
1572 G. Altarelli, G. Parisi, Asymptotic Freedom in Parton Language *Nucl. Phys.* **B126**, 298 (1977)
1503 S. Coleman, E. Weinberg, Radiative Corrections as the Origin Of Spontaneous Symmetry Breaking *Phys. Rev.* **D7**, 1888 (1973)
1491 H.D. Politzer, Reliable Perturbative Results for Strong Interactions? *Phys. Rev. Lett.* **30**, 1346 (1973)
1478 M.A. Shifman, A.I. Vainshtein, V.I. Zakharov, QCD and Resonance Physics *Nucl. Phys.* **B147**, 385 (1979)
1474 A.A. Belavin, A.M. Polyakov, A.B. Zamolodchikov, Infinite Conformal Symmetry in 2-D Quantum Field Theory *Nucl. Phys.* **B241**, 333 (1984)
1472 G. 't Hooft, Computation of Quantum Effects Due to 4-D Pseudoparticle *Phys. Rev.* **D14**, 3432 (1976)
1390 P. Candelas, G. T. Horowitz, A. Strominger, E. Witten, Vacuum Configurations for Superstrings *Nucl. Phys.* **B258**, 46 (1985)
1381 G. 't Hooft, Symmetry Breaking Through Bell-Jackiw Anomalies *Phys. Rev. Lett.* **37**, 8 (1976)
1371 D.J. Gross, F. Wilczek, Ultraviolet Behavior of Non-Abelian Gauge Theories *Phys. Rev. Lett.* **30**, 1343 (1973)
1348 A.M. Polyakov, Quantum Geometry of Bosonic Strings *Phys. Lett.* **B103**, 207 (1981)
1341 S.L. Adler, Axial-Vector Vertex in Spinor Electrodynamics *Phys. Rev.* **177**, 2426 (1969)
1340 Y. Nambu, G. Jona-Lasinio, Dynamical Model of Elementary Particles *Phys. Rev.* **122**, 345 (1961)
1288 E. Eichten, I. Hinchliffe, K. Lane, C. Quigg, Supercollider Physics *Rev. Mod. Phys.* **56**, 579 (1984)
1254 G. 't Hooft, M. Veltman, Regularization And Renormalization of Gauge Fields *Nucl. Phys.* **B44**, 189 (1972)
1253 J.J. Hernandez, et al. (Particle Data Group), Review of Particle Properties *Phys. Rev.* **D45**, S1 (1992)
1250 A. H. Guth, Inflationary Universe: Possible Solution To Horizon and Flatness Problems *Phys. Rev.* **D23**, 347 (1981)
1236 A.A Belavin, A.M. Polyakov, A.S. Schwartz, Yu.S. Tyupkin, Pseudoparticle Solutions of Yang-Mills Equations *Phys. Lett.* **B59**, 85 (1975)
1232 A. De Rujula, H. Georgi, S.L. Glashow, Hadron Masses in a Gauge Theory *Phys. Rev.* **D12**, 147 (1975)
1220 J.J. Hernandez, et al. (Particle Data Group), Review of Particle Properties *Phys. Lett.* **B239**, 1 (1990)
1175 D.J. Gross, J.A. Harvey, E. Martinec, R. Rohm, Heterotic String Theory 1 *Nucl. Phys.* **B256**, 253 (1985)
1117 J.J. Aubert, et al., Experimental Observation of a Heavy Particle J *Phys. Rev. Lett.* **33**, 1404 (1974)
1100 A. Chodos, R.L. Jaffe, K. Johnson, C.B. Thorn, V.F. Weisskopf, A New Extended Model of Hadrons *Phys. Rev.* **D9**, 3471 (1974)
1100 G. 't Hooft, Magnetic Monopoles in Unified Gauge Theories *Nucl. Phys.* **B79**, 276 (1974)

THE FIRST LIST shows the articles most popular in the past three years, while the second displays all-time favorites. Both lists were compiled on December 31, 1994. The all-time list reads like a Who's Who of high-energy physics. Steven Weinberg's article *A Model of Leptons* is by far the most popular work in high-energy physics. The most fruitful period in this field, according to the list, was the early seventies: ten articles from the list were published in just two years, 1973 and 1974. A paper had to have at least 1100 citations to get to the 'all-time' top-30 list. If your paper did not cross this magic boundary, but has more than, say, 250 citations, it is still in a very exclusive company: a study shows that there are only about 180 papers with 500 or more citations in the HEP database, and only about 600 papers with more than 250 citations. Compare this to the total number of published high-energy physics papers, which, according to some estimates, may be close to 100,000.*

* *An extended version of this article may be found on the World Wide Web, at http://www-slac.slac.stanford.edu/find/top40.html.*

Hrvoje Galić is a theoretical physicist, working now as a SPIRES specialist in the SLAC library. None of his theoretical works has made it to the top 1000 list.

Astrophysics in 1994

by VIRGINIA TRIMBLE

The author takes typewriter, notebook, and eraser in hand to review, in brief and prejudiced fashion, a few of the highlights of the astronomical year.

BACK IN 1990, the then-new editor of *Publications of the Astronomical Society of the Pacific*, Howard Bond, asked me to undertake an overview of everything that had appeared in the astronomical literature over the past 12 months, with the intention that this should become an annual event, until either he or I was lynched by the uncited.

Papers called "Astrophysics in 1991," 1992, and 1993 in due course appeared, and Ap94 has just been handed over to the editor (or at least the US post office). It touches on something like 81 topics, a subset of which seemed like enough fun to be worth sharing with *Beam Line* readers. Incidentally, just in case you have been wondering about the author carrying three awkward things at once, it is clear that, since she has two left hands, the total must be at least three.

THE DEMISE OF THE JOVIAN DINOSAURS

On 16 July, 1994 fragments of disrupted comet (or whatever) Shoemaker-Levy 9 began hitting Jupiter. Visitors to the planet after that date are guaranteed not to find any dinosaurs living there, by analogy with the damage done to the fauna of the terrestrial Mesozoic era by an asteroid/comet impact about 60 million years ago. Admittedly, I am pretty sure that Jovian visitors before July 16 would not have found any dinosaurs either.

Some more controversial questions can also be addressed once the images and spectra of the impact events have been fully analyzed. These include the chemical composition of the layers of Jupiter that were kicked up (why so little water; how much of sulfur and its compounds?) and whether the impacting fragments belonged to a comet in the traditional sense of dirty snowball or something more like an asteroid, in the sense of ice-polluted rocky stuff. Even more interesting are the sociological questions. Why did comet experts so greatly underestimate (at least in public) how spectacular the collisions would be? The easy, and perhaps correct, answer is "once burned, twice shy," for overestimates of what casual observers might see of Comet Halley back in 1986 had done nobody any good.

Another issue where political considerations outweigh purely scientific ones is what, if anything, the event will mean for the progress of searches for asteroids that pass close to the earth and the development of technology to modify their orbits. Inevitably, many astronomers resent the thought that money that could be spent on useful

NASA

An image of Jupiter by NASA's Hubble Space Telescope, revealing the impact sites of fragments "D" and "G" from Comet Shoemaker-Levy 9. The large feature was created by the impact of fragment "G" on July 18, 1994 at 3:28 a.m. EDT. The smaller feature to the left of the fragment "G" impact site was created on July 17, 1994 at 7:45 a.m. EDT by the impact of fragment "D". The "G" impact has concentric rings around it, with a central dark spot 1550 miles in diameter. The dark thick outermost ring's inner edge has a diameter of 7460 miles—about the size of the Earth. The impact sites are located in Jupiter's southern hemisphere at a latitude of 44 degrees.

topics like asymptotic giant branch stars and Seyfert galaxies might be diverted to comet and asteroid patrols. In fact, these latter are also capable of yielding information about the numbers of very small bodies in the outer solar system, their likelihood of collisional disruption, and the balance between rocks and ices in these objects that are the most nearly pristine samples left from when the solar system formed. This is interesting stuff in its own right, and I am prepared to give up a few of my white dwarf X-ray photons and half a HIPPARCOS (astronometric satellite) star in return for an

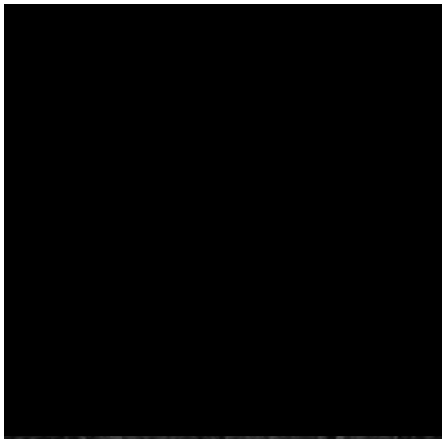

NASA

Wide Field Camera (Hubble Space Telescope) image of the core of nearby active galaxy M87. Spectroscopic data also exist. The signature of the central black hole is that both the surface brightness of the image and the velocity dispersion shown in the spectra increase rapidly toward a sharp, central cusp. The alternative explanation, in terms of a central very dense cluster of stars, is less likely because the cluster would rather quickly merge into a black hole. (Image courtesy of NASA.)

earth-crossing asteroid with surface composition like that of some of the commoner meteorites.

MY BLACK HOLE IS BIGGER THAN YOUR BLACK HOLE

And M87's is bigger than just about everybody's. Most astronomers have accepted for at least a couple of decades that gravity can triumph over the other three forces and produce configurations inside their Schwarzschild horizons in at least two contexts. The first is at the death of very massive stars, whose cores collapse beyond neutron star densities. The other is at the centers of relatively massive galaxies, where stellar and gaseous debris, deprived of its fair share of angular momentum, will pile up, until, sometimes, $R < 2\ GM/c^2$, and even Houdini could not get out.

Such a black hole, with a mass of 10^6–10^{10} times that of a single star and accreting gas from its surroundings, is the standard model accounting for high luminosity, small size, and rapid variability in the active galaxies called quasars, radio galaxies, Seyferts and so forth. Statistical considerations indicate that the active phase should last 1 percent or less of the age of the universe, turning off when there is no longer much gas left in orbits where it can be accreted. Thus many seemingly normal galaxies ought to harbor massive black holes in their cores, left from their misspent youth.

Three interesting examples began giving up their secrets in 1994. First, M87, a nearby active, radio-emitting galaxy, was imaged with better-than-ever angular resolution by the Hubble Space Telescope. The light distribution, mass distribution, and stellar velocity dispersion all show sharp central peaks. These were known from earlier ground-based data, but the higher-resolution HST measurements make it much harder to imitate a black hole with a dense star cluster or other impostor. The implied mass is 2–3 billion solar masses, hefty but still small compared to a whole galaxy of $10^{11–12}$ solar masses.

Second comes NGC 4258, a totally boring galaxy that has not made the cover of *Science News*. But its center is studded with water maser sources, whose locations and velocities, determined with radio interferometers, look very much like a Keplerian disk around a central point mass of 10^7 solar masses, just what you would expect in a former, bright Seyfert galaxy. Other normal galaxies, like NGC 3115, seem to have billion solar mass, dead quasar, central masses.

Finally the presence or absence of a modest black hole in our own Milky Way has been under acrimonious discussion since at least the early 1970s. No final answer is in. But a gaggle of faint stars (seen as infrared sources) are grouped close enough to the center that, once their velocity dispersion has been measured, the issue will be settled. This has to be done by repeated imaging over several years, to follow their motions on the plane of the sky. Preliminary data say, yes, there is a million solar mass black hole. A firmer YES (or NO) should be possible by about 1997. Meanwhile, the absence of X-rays and other signatures of activity at the center of the Milky Way has to be blamed on lack of gas to accrete.

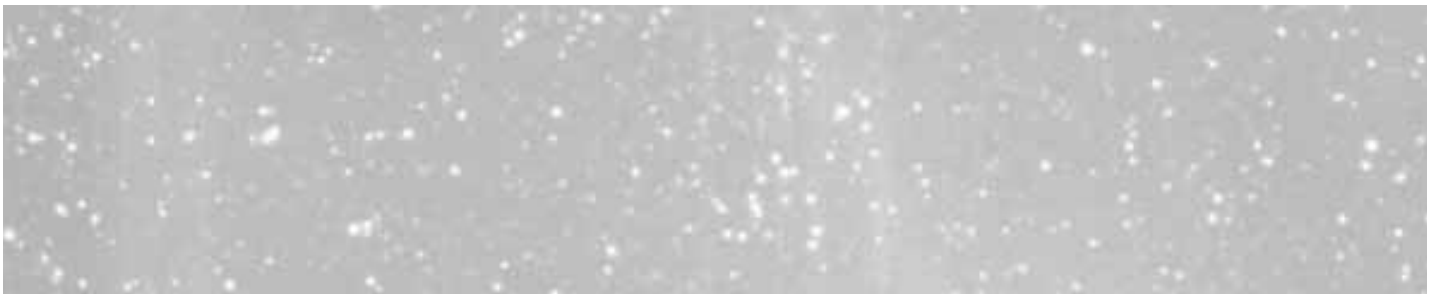

THE HELIUM GUNN-PETERSON EFFECT, PRIMORDIAL DEUTERIUM, AND BIG BANG NUCLEOSYNTHESIS

The big questions here are (a) how much stray gas is there between the galaxies, and is it a significant contributor to closing the universe? (b) how much deuterium (as well as He^3, He^4, and Li^7) was made in the early universe? and (c) do these fit together sensibly in terms of the nuclear reactions that turned the early proton-neutron-electron soup into simple elements?

If you wish to add a fourth, minor question, "Who was Dr. Helium?", the answer is that he was a close relative of Mr. Metro (of Metro-Goldwyn-Mayer). Gunn and Peterson were the then-graduate students who, in 1965, pointed out that absence of trough-like Lyman-alpha absorption in the spectra of quasars with redshifts large enough to move 1216 Å into the visible spectrum set a very stringent limit on the amount of hydrogen gas between the galaxies. Gunn-Peterson absorption by neutral hydrogen has not been seen from that day to this (Friday), and the limit has become so stringent that highly ionized gas seems the only believable explanation. This has now been seen, in the form of trough-like absorption at the wavelength absorbed by ionized helium when its sole remaining electron is excited from ground to first excited level. The data come from the high resolution spectrograph on the 10-meter Keck telescope (currently the world's largest at optical wavelengths) and suggest an intergalactic medium whose density is 1 percent or less of that needed to close the universe, but which might be interesting in terms of the total amount of baryonic material around.

The deuterium-to-hydrogen ratio is the probe *par excellence* of baryon density in the early universe. Qualitatively, it's easy to see why. If there are lots of n's, p's, and d's floating around, everybody finds somebody and it all burns through to helium. If not, not. We have been living for a generation happily with a primordial $D/H = 1–4\times10^{-5}$, as implied by solar system measurements, nearby interstellar gas, and maybe a few other samples. Great, therefore, was the consternation when two separate groups this spring reported that they had seen $D/H = 2.5\times10^{-4}$ in the form of a greatly-redshifted pair of absorption lines in the light of a distant quasar. Preprints fluttered, because getting that much deuterium out requires a perilously low baryon density (you want, at least, to be able to make the stars and galaxies we see!). But the two groups were looking at the same lines in the same quasar (albeit with different telescopes), and suspicion has been rising that what they saw was not deuterium in a dense cloud at all, but rather ordinary hydrogen in a much less dense cloud that just happened to have the bad luck to be moving at a speed to put its Lyman-alpha line at the wavelength where the deuterium line would be in the dense cloud. Rumors abound of a different distant quasar with a line that is plausibly deuterium at the expected abundance. Wavelength coincidences cannot happen often, so detection of just a few more candidate lines will settle the issue.

Meanwhile, some pundits had hailed the mere detection of helium and/or deuterium at large redshifts as triumphal confirmation of the standard big bang picture of the early universe. Frankly, I had ceased to have any doubts about this about the time I gave up reading Winnie the Pooh for *Beam Line*.

TWINKLE, TWINKLE LITTLE MACHO

Another of the highlights of the year also has some bearing on the issue of how much baryonic material there is in the universe. Or at least it might have. At the moment, one feels more as if stars have been rediscovered by a very difficult method. The general idea (put forward by Bohdan Paczyński in 1986) is that, if the dark matter in the halo of the Milky Way consists of discrete objects with masses of anything from 10^{-10} to 10^{+6} solar masses, these will cause gravitational lensing amplification of background stars when they pass between us and the background. If you pick a very dense background region (a nearby companion galaxy or the center of the Milky Way), you need watch carefully only a few

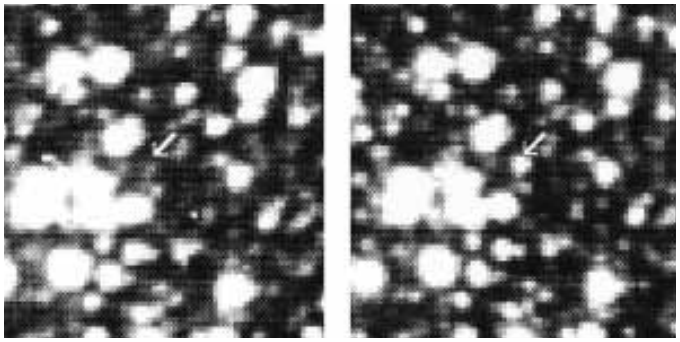

Gravitational lensing event recorded by OGLE (Optical Gravitational Lensing Experiment) collaboration. The arrow in the left image points to a distant star at its normal brightness. In the right hand image, we see the star greatly brightened because a nearer star, too faint to see, has passed in front, magnifying the distant one. (Images courtesy of A. Udalski, M. Szymański, and Mario Mateo.)

million stars to have a good chance of catching one lensing event per year.

MACHO is an acronym for MAssive Compact Halo Object and also the name of one of the three collaborations that started to look for lensing events in 1991 and have now collectively reported many dozens (though only a few are in the archival literature). Several surprises have surfaced. First, the event rate toward a nearby galaxy, the Large Magellanic Cloud, is only about a third of what the searchers were expecting. The dark matter in the halo of our galaxy is not all in the form of MACHOs in the accessible mass range—and, therefore, at a much lower confidence level, probably not all baryonic.

Second, the event rate toward the galactic center is about three times the predicted rate. This means that there are more compact objects somewhere along the line of sight than we thought there were. The explanation apparently involves a non-spherical, bar-like component in the distribution of stars near the galactic center, with one end of the bar intruding into the search fields. Such bars are common in other spiral galaxies (and independent evidence for ours exists in the form of non-circular gas velocities in the region).

Third, the average properties of the events are not quite what was hoped for. One of the survey teams, called OGLE, started out looking toward the galactic center because that way they could be sure of seeing something eventually, if the technique and calculations were right. There are, after all, lots of massive compact objects in the galactic disk and bulge between us and the center. They are called stars. And this seems to be what the projects have discovered. The most probable masses (only statistical determinations are possible from the duration and amplification of lensing events) for most lenses are those of small stars, not substellar objects or brown dwarfs.

The three projects are producing enormous quantities of astronomical spin-off. I have already mentioned the demonstration that the Milky Way is a barred spiral. The MACHO group has seen a new class of variable stars that they call blue bumpers (given the PC level of the collaboration name, I wouldn't be surprised if these started out as "blue bump and grind stars!"). And OGLE is producing an enormous catalog of known and unknown variable stars, as well as having found independent evidence for the new galaxy mentioned in the next section.

Despite the frivolous tone of most of these remarks, I would like to record here enormous admiration for the persistence, mechanical ingenuity, and prompt data release of the three survey groups.

Not quite incidentally, a number of other searches for brown dwarfs in the last few years, by a wide range of other methods, have yielded mighty slim pickin's.

IGI

The Milky Way belongs to a small, local group of galaxies, called (with that enormous creativity of nomenclature for which astronomers are world renowned) the Local Group. The other members are a second large spiral galaxy (the Andromeda nebula, or M31), a smaller spiral (M33) and more than two dozen dwarfs, some with gas, and some without. The inventory keeps growing, and the latest recruit is a dwarf spheroidal galaxy, meaning no gas and not many more than 10^{6-7} stars, that

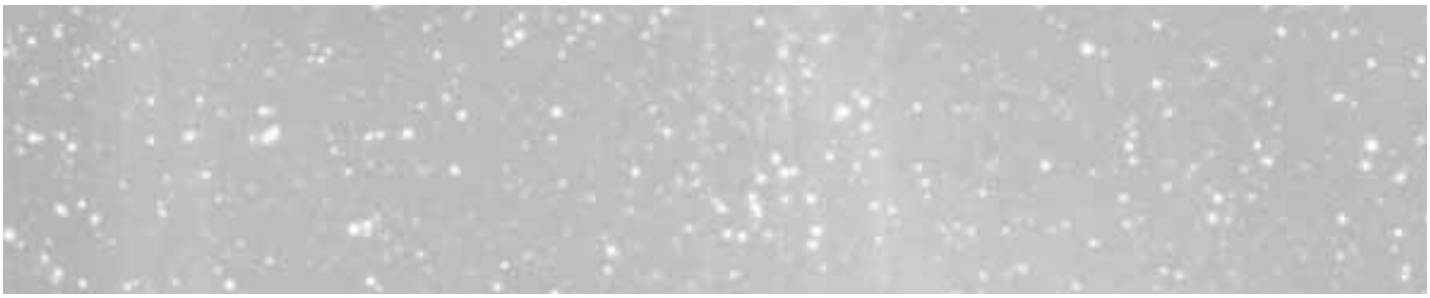

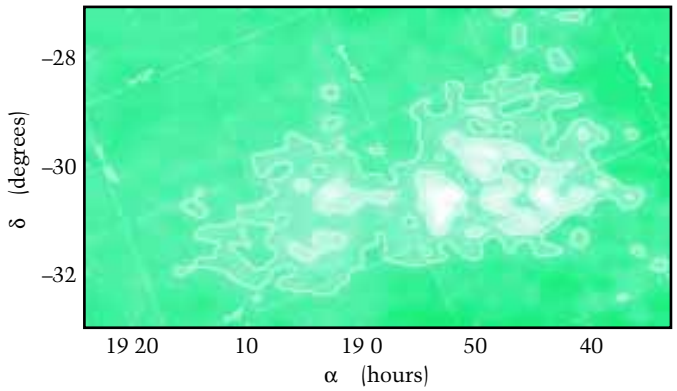

An isodensity map of the newly discovered dwarf galaxy in the constellation of Sagittarius. (Courtesy of Rodrigo Ibata, Institute of Astronomy.)

has the bad luck to be almost exactly on the far side of the galactic center from us, and close in at that. As a result, the new galaxy is quite difficult to see or photograph, and is in the process of being torn apart by tidal forces of the Milky Way itself.

The discoverers, Ibata, Gilmore, and Irwin (whose initials are NOT the official name of the galaxy) found our new neighbor accidentally, in a project intended to clarify the kinds of stars that make up the central regions of our own galaxy. It shows up independently in star counts by the OGLE group (above, and yes that is their official name). One can't help suspecting that such undiscovered dwarf galaxies may be fairly common. Even the ones found by Hubble early in the 20th century are hard to recognize until someone tells you what to look for. Slightly larger dwarf spheroidals are known to be the single commonest kind of galaxy in rich clusters like that seen past the constellation Virgo.

EINSTEIN IS DEAD

Not precisely news, you will say. But this was the headline in a nameless Pasadena newspaper (we have heard rumors of a morphological class called lawyers who take an interest in such matters) some 20 years ago, when radio astronomers reported that they had seen bits and pieces of compact, distant quasars and radio galaxies that seemed to be moving across the sky at 2–10 times the speed of light. No alarm was called for even then. The effect had been predicted (see top figure on next page) a few years before, and is a projection along the line of sight of relativistically beamed gas moving at 90 percent or so of the speed of light. From discovery in 1972 until this year, all were in distant galaxies.

The new development is that our own galaxy also harbors at least two superluminal sources. They are not associated with our rather feeble galactic center (with or without its black hole). Rather, the beamed jets are accelerated by neutron stars or black holes in binary systems that reveal themselves as flaring X-ray sources. The rapidly-moving jet tips (or whatever) are best studied as radio sources, and once again it is radio astronomers who have shown that what was first called "an X-ray nova in Scorpius" has a superluminal component. Press conferences on it were still being held when a second X-ray flare source started doing the same sort of thing in August. It is hard to escape the conclusion

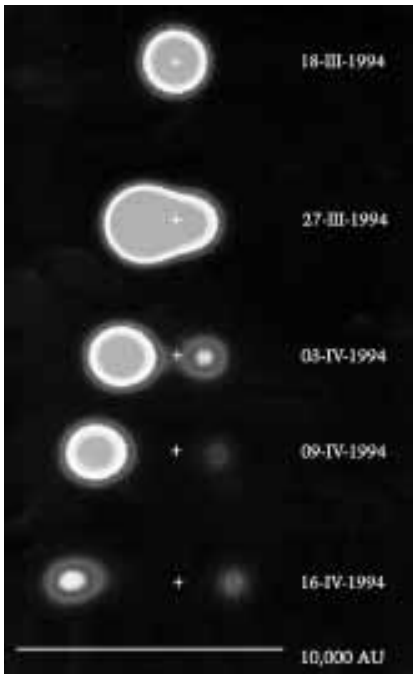

Sequence of radio maps of X-ray nova GRS 1915+105 from March and April 1994. The source seems to be expanding rapidly, from a single blob to two widely separated ones, with components separating at 1.9 times the speed of light. This is a sort of optical illusion attributable to motion at about 0.92 c, at an angle of 70° to our line of sight. [Adapted from I. F. Mirabel and L. F. Rodriguez, Nature, 371, *46 (1994).]*

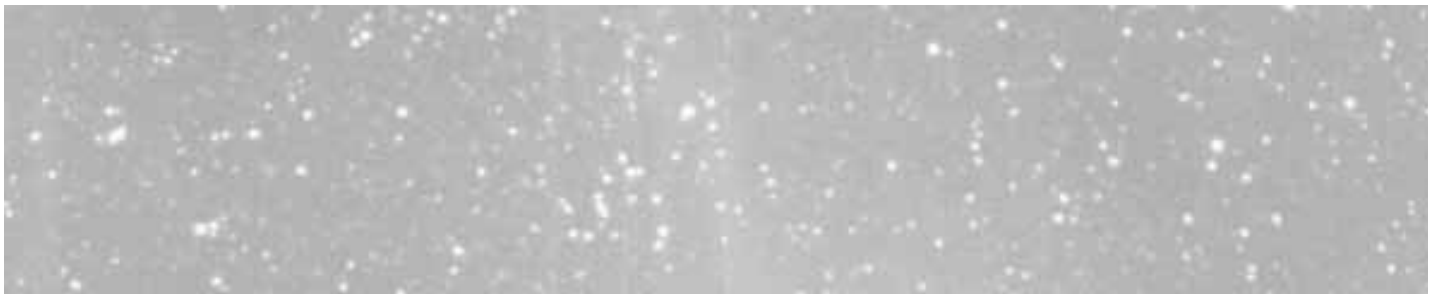

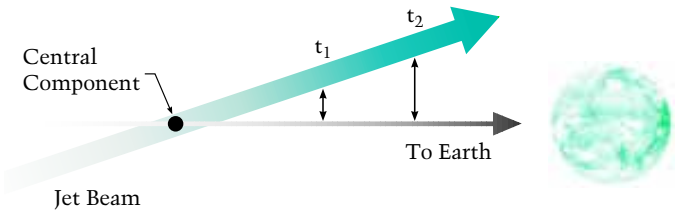

Because the jet is moving quickly and almost directly towards us, a photon emitted at t_2 doesn't have to travel as far as a photon emitted at t_1 and so arrives very soon after the first one. Thus it looks as if the emitting bit of gas had moved across the plane of the sky very quickly. The other jet, heading away from us, is Doppler-faintened and normally not seen, though its effects on its surroundings may be.

that these, like dwarf spheroidal galaxies, are very common, once you know how to look for them.

"A FAINT LUMINOUS HALO THAT MAY TRACE THE DARK MASS DISTRIBUTION OF SPIRAL GALAXY NGC 5907"

That's the title of the paper, published in *Nature* this fall, and it says it all. Penny Sackett and her colleagues have not necessarily seen dark matter. But they have seen a faint glow around this galaxy with a distribution that looks like the mass density distribution of a typical dark halo, that is, something that scales like R^{-2} rather than R^{-3} or steeper, the way the visible star distribution does. They had no color information about the light as they (and we) went to press. But if all the light and all the mass of the halo of this particular galaxy came from a single class of known astronomical object, then the objects would be faint, low-mass stars, very much like the ones that are turning up as lenses in the gravitational lensing (MACHO) searches described a page or two back.

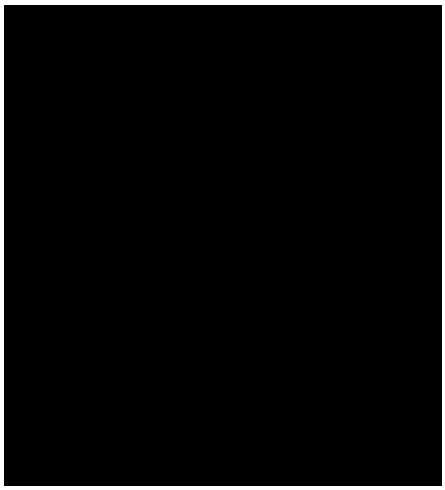

Natonal Optical Astronomy Observatories

CCD image (taken with a 36" telescope) of the edge-on spiral galaxy NGC 5907. The data, in digitized form, show that, in addition to the obvious, very flat spiral disk, there is a power-law component, with luminosity density proportional to $r^{-2.2}$, extending at least 6000 parsecs (2×10^{22} cm) perpendicular to the disk. This is the sort of density law that dark halos must have in order to account for the dynamics of spiral galaxies. (Courtesy of Penny Sackett.)

AND ALL THE REST

"Astrophysics in 1994" cites about 400 papers, culled from nearly 20 times that many read by my co-author and me during the "reference year" 1 October 1993 to 30 September 1994. From the 81±x topics discussed there, I have picked about nine, and given even them fairly short shrift. Were it not for the impiety, one would be reminded of the time when Rabbi Hillel was asked to explain The Law while standing on one foot. He did so, saying "That which is hateful to you, do not do to another. All the rest is commentary. Now go read the commentary." In less lofty fashion, the archival literature of astronomy and physics repays reading!

Suggestions for Further Reading

"Astrophysics in 1994" by V. Trimble and P.J.T. Leonard is scheduled to appear in the January 1995 issue of *Publications of the Astronomical Society of the Pacific*. It contains the original references to the items mentioned here, and many others.

CONTRIBUTORS

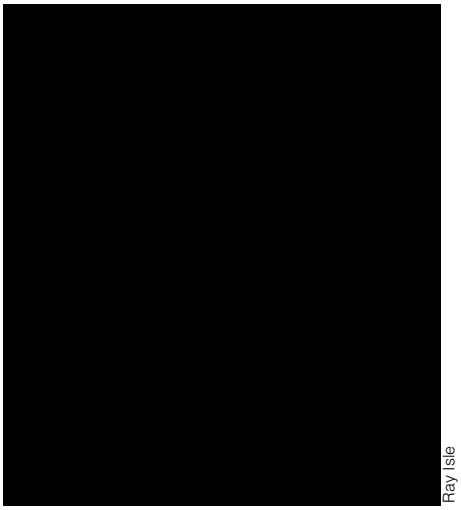

Ray Isle

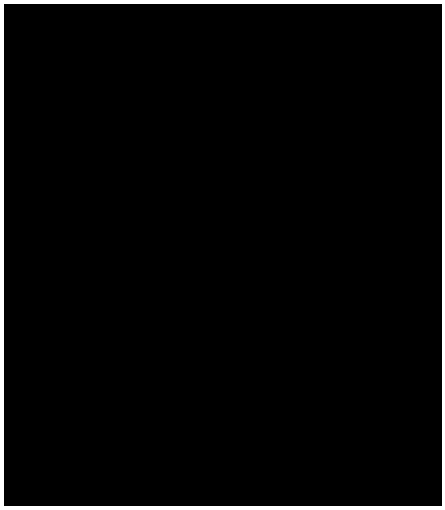

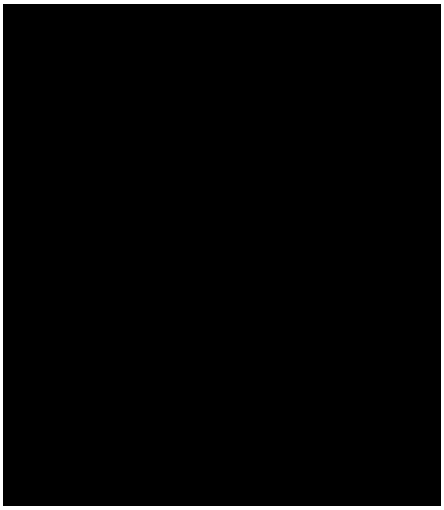

Tony Johnson is a staff physicist at the Stanford Linear Accelerator Center. He has a D. Phil in Nuclear Physics from Oxford University where he did his graduate work with the European Muon Collaboration at CERN. Since graduating in 1984 he has worked at SLAC on the ASP experiment at PEP and on the SLD experiment at the SLAC linear collider, employed first by MIT, then by Boston University, and most recently by SLAC.

He first realized the potential of the World Wide Web after seeing a presentation by Tim Berners-Lee in early 1992 and is the author of one of the first X-windows-based WWW browsers called Midas. He spends all his spare time surfing the Web reading theoretical physics papers and never wastes any time reading *Dr. Fun*, *Netboy* or *Dilbert*, especially not *Dilbert*.

John Bahcall was awarded the 1994 Heinemann Prize for his work on solar neutrinos—a field which he and Ray Davis have worked to develop for much of the past 32 years. He is the author of the book **Neutrino Astrophysics**. A member of the National Academy of Sciences, of Academia Europea, and a recipient of NASA's Distinguished Public Service Medal for his work on the Hubble Space Telescope, Bahcall is a past president of the American Astronomical Society and the Chair of the National Academy of Sciences Decade Survey Committee for Astronomy and Astrophysics. Trained as a physicist, he is Professor of Natural Sciences at the Institute for Advanced Study, where he is working on HST images of nearby luminous quasars and improvements in solar neutrino calculations.

Robert A. Scott is Professor of Chemistry and Biochemistry and Co-director of the Center for Metalloenzyme Studies at the University of Georgia in Athens. After receiving a Ph.D. at the California Institute of Technology, he spent two years as an NIH postdoctoral fellow at Stanford University with Keith Hodgson, where he became involved in the use of X-ray absorption spectroscopy at SSRL for the study of metals in biology. In addition to continuing this interest throughout semiannual visits to SSRL, his present research emphasis is on the molecular determinants of metalloprotein stability and redox chemistry and structure/function relationships in metalloenzymes. Scott was a recipient of the National Science Foundation Presidential Young Investigator Award, 1985–1990.

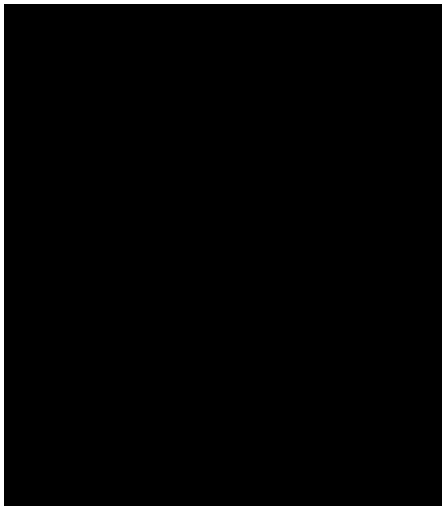

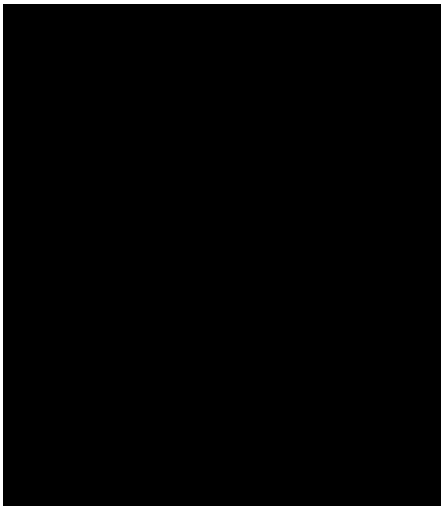

P. Waloschek

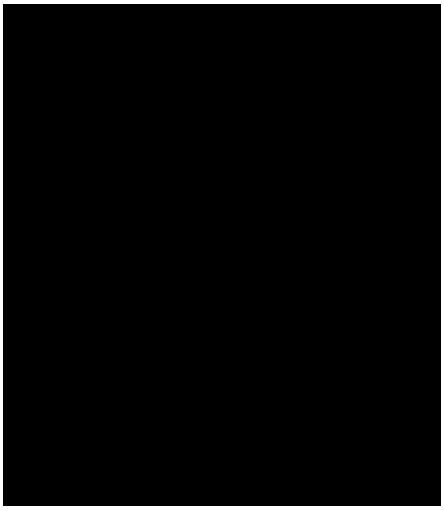

Educated at Tübingen and Hamburg, Günter Wolf is an experimental physicist working at DESY (since 1961) and SLAC (1967–1970 and 1984–1985) on hadron- and photoproduction, deep inelastic scattering, electron-positron annihilation, and now on electron-proton collisions. He has been the spokesman of several experiments, such as the laser-induced polarized photon experiment at SLAC, the TASSO experiment at PETRA, and the ZEUS experiment at HERA.

Franz Eisele, now professor of physics at the University of Heidelberg, was the spokesman of the H1 collaboration for six and a half years from the start of construction up to the first year of data taking. His research concentrated on lepton-scattering experiments, first at CERN with high energy neutrinos from 1976 to 1984, and later at HERA studying the structure of weak interactions, measuring parton distributions and testing QCD. Moreover, he has also been engaged in CP violation experiments in the neutral kaon system at CERN, and more recently in the *B*-meson system at HERA.

Virginia Trimble first gave an invited talk on a subject about which others knew far more, as an emergency substitute for an injured colleague, at an IAU symposium in 1970. She hasn't looked back since (except when writing historic reviews), and, in contrast to the normal, specialist researcher's goal of knowing absolutely everything about very little, she has been striving to know very little about absolutely everything. At least the first part of this has clearly been achieved. She can be reached from July to December each year at the Astronomy Department of the University of Maryland in College Park and from January to June each year at the newly christened Department of Physics and Astronomy of the University of California, Irvine.

DATES TO REMEMBER

Mar 13–18	Strings 95: Future Perspectives in String Theory, Los Angeles, CA (Dept. of Physics and Astronomy, University of Southern California, Los Angeles, CA 90089-0484 or STRINGS@PHYSICS.USC.EDU).
Mar 15–18	Spectroscopies in Novel Superconductors, Stanford, CA (Katherine Cantwell, SSRL, MS 69, Box 4349, Stanford, CA 94309-0210 or K@SLAC.STANFORD.EDU).
Apr 8–13	10th Workshop on Photon-Photon Collisions (Photon 95), Sheffield, England (Prof. F. Combley, Dept. of Physics, University of Sheffield, Sheffield S3 7RH, England or COMBLEY@CERNVM.CERN.CH).
Apr 18–21	General Meeting of the American Physical Society (APS), Washington, DC (The American Physical Society, 1 Physics Ellipse, College Park, MD 20740-3844).
May 1–5	IEEE Particle Accelerator Conference (PAC 95), Dallas, TX (Stanley Schriber, LANL AOT, MS H811, Los Alamos, NM 87545 or SSCHRIBER@LANL.GOV).
May 9–13	10th Topical Workshop on Proton-Antiproton Collider Physics, Batavia, IL (C.M. Sazama, Fermilab, MS 122, PO Box 500, Batavia, IL 60510 or SAZAMA@FNALV.FNAL.GOV).
July 10–14	6th International Conference on Hadron Spectroscopy (Hadron 95), Manchester, UK (Dept. of Physics and Astronomy, University of Manchester, Manchester M13 9PL, UK or HADRON95@V2.PH.MAN.AC.UK).
July 10–21	XXII SLAC Summer Institute on Particle Physics: The Top Quark and the Electroweak Interaction, Stanford, CA (L. DePorcel, SLAC, PO Box 4349, Stanford, CA 94309).
July 24–28	16th Annual Meeting, TeX Users Group: TUG '95: TeX Goes to Florida, St. Petersburg Beach, FL (TeX Users Group, PO Box 869, Santa Barbara, CA 93102 or TUG95C@SCRI.FSU.EDU).
July 27–29	Workshop on the Search for New Elementary Particles, Trieste, Italy (F. Hussain, ICTP Workshop on the Search for New Elementary Particles, PO Box 586, I-34100, Trieste, Italy or SMR864@ICTP.TRIESTE.IT).
July 31–Sep 6	International Europhysics Conference on High Energy Physics (HEP 95), Brussels, Belgium (European Physics Society, PO Box 69, CH-1213 Petit-Lancy 2, Switzerland or EPNEWS@CERNVM.CERN.CH).